

AD-A007 353

DAVID W TAYLOR NAVAL SHIP RESEARCH AND DEVELOPMENT CE--ETC F/G 13/11  
FINITE ELEMENT ANALYSIS OF PIPING TEES.(U)

JUN 80 A J QUEZON, G C EVERSTINE, M E GOLDEN

UNCLASSIFIED

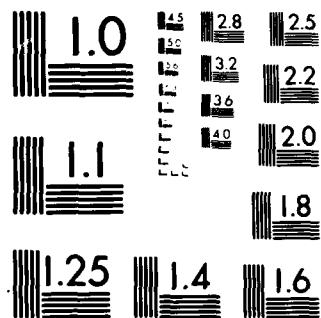
DTNSRDC/CMLD-80/11

NL

For 1  
of 1




END  
DATE  
FILMED  
9-80  
DTIC



MICROCOPY RESOLUTION TEST CHART

NATIONAL BUREAU OF STANDARDS-1963-A

DTNSRDC/CMLD-80/11

LEVEL

(12)

**DAVID W. TAYLOR NAVAL SHIP  
RESEARCH AND DEVELOPMENT CENTER**

Bethesda, Md. 20084



ADA 087353

FINITE ELEMENT ANALYSIS OF PIPING TEES

by

Antonio J. Quezon, Gordon C. Everstine, and Michael E. Golden

APPROVED FOR PUBLIC RELEASE: DISTRIBUTION UNLIMITED.

DTIC  
ELECTE  
AUG 1 1980  
S A D

COMPUTATION, MATHEMATICS, AND LOGISTICS DEPARTMENT  
DEPARTMENTAL REPORT

DDC FILE COPY

ne 1980

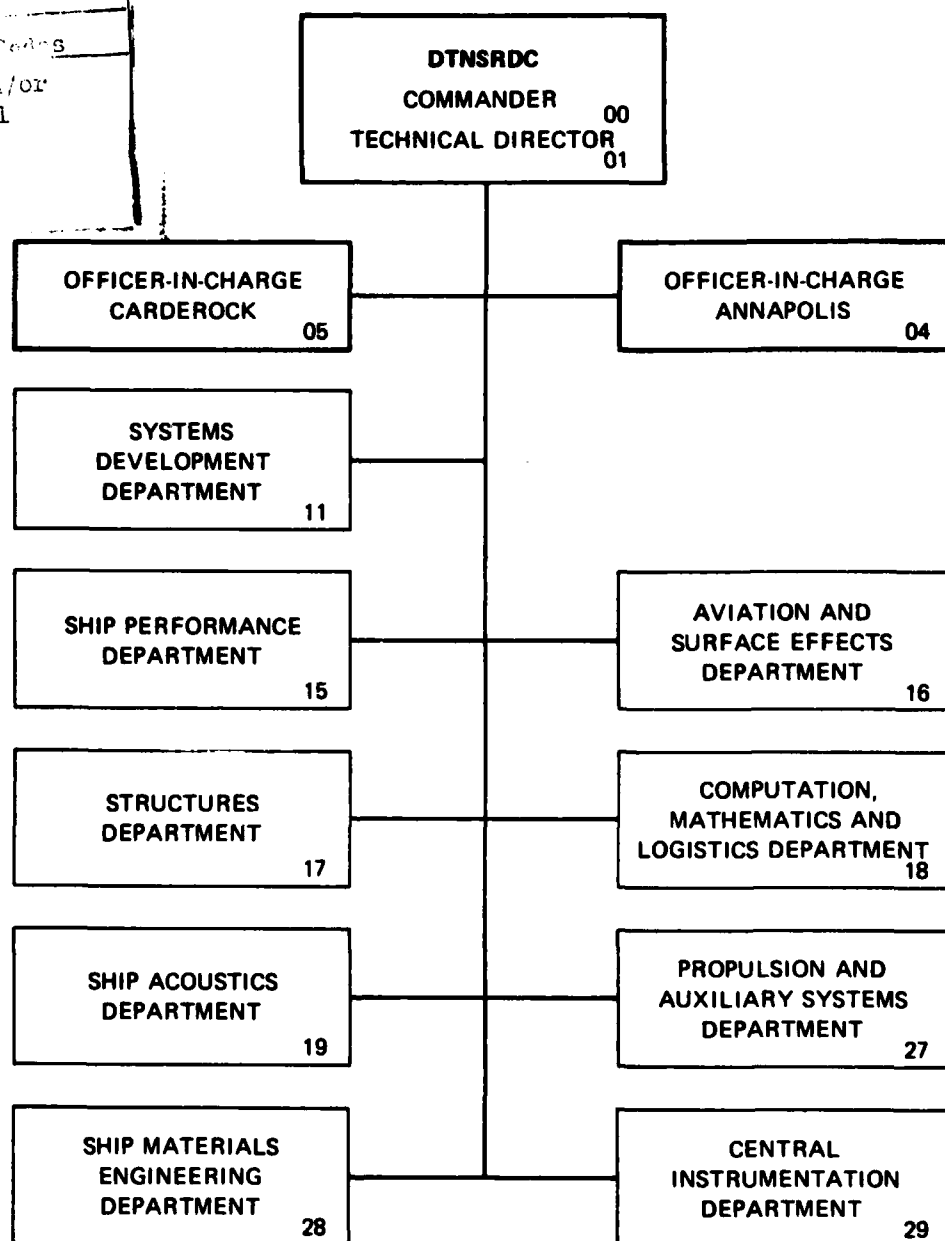
DTNSRDC/CMLD-80/11

FINITE ELEMENT ANALYSIS OF PIPING TEES

80 7 30 042

Accession stamp	
NTIS	<input checked="" type="checkbox"/>
DDC	<input type="checkbox"/>
Unac.	<input type="checkbox"/>
Jan.	<input type="checkbox"/>
By _____	
Dist _____	
Asst. Dir. _____	
Special _____	
Dist	<input checked="" type="checkbox"/>

# MAJOR DTNSRDC ORGANIZATIONAL COMPONENTS



UNCLASSIFIED

SECURITY CLASSIFICATION OF THIS PAGE (When Data Entered)

REPORT DOCUMENTATION PAGE		READ INSTRUCTIONS BEFORE COMPLETING FORM
1. REPORT NUMBER DTNSRDC/CMLD-89/11	2. GOVT ACCESSION NO. AD-A087 353	3. RECIPIENT'S CATALOG NUMBER
4. TITLE (and Subtitle) FINITE ELEMENT ANALYSIS OF PIPING TEES	5. TYPE OF REPORT & PERIOD COVERED Final rept. Oct 1979 - Jun 1980	6. PERFORMING ORG. REPORT NUMBER
7. AUTHOR(s) Antonio J. Quezon, Gordon C. Everstine, Michael E. Golden	8. CONTRACT OR GRANT NUMBER(s) 4654348	
9. PERFORMING ORGANIZATION NAME AND ADDRESS David W. Taylor Naval Ship Research and Development Center Bethesda, Maryland 20084	10. PROGRAM ELEMENT, PROJECT, TASK AREA & WORK UNIT NUMBERS Program Element 63561N Task Area S8348001 Work Unit 1-2740-163	
11. CONTROLLING OFFICE NAME AND ADDRESS	12. REPORT DATE Jun 1980	13. NUMBER OF PAGES 48
14. MONITORING AGENCY NAME & ADDRESS (if different from Controlling Office)	15. SECURITY CLASS. (of this report) UNCLASSIFIED	15a. DECLASSIFICATION/DOWNGRADING SCHEDULE
16. DISTRIBUTION STATEMENT (of this Report)  APPROVED FOR PUBLIC RELEASE: DISTRIBUTION UNLIMITED.		
17. DISTRIBUTION STATEMENT (of the abstract entered in Block 20, if different from Report)		
18. SUPPLEMENTARY NOTES		
19. KEY WORDS (Continue on reverse side if necessary and identify by block number)  Piping tee                      NASTRAN Tee analysis                    CORTES Finite elements		
20. ABSTRACT (Continue on reverse side if necessary and identify by block number)  Finite element analyses were performed for a 24" x 24" x 10" schedule 40 carbon steel piping tee subjected to five orthogonal forces, six orthogonal moments, and internal pressure. The NASTRAN and CORTES/SA computer programs were used to compute displacements and normalized principal stresses for four finite element models. (CORTES/SA is a special purpose finite element analysis program for tee joints developed at the University of California at Berkeley.)		

(Continued on reverse side)

DD FORM 1 JAN 73 1473

EDITION OF 1 NOV 65 IS OBSOLETE  
S/N 0102-LF-014-6601

UNCLASSIFIED

SECURITY CLASSIFICATION OF THIS PAGE (When Data Entered)

406847

JCB

UNCLASSIFIED

SECURITY CLASSIFICATION OF THIS PAGE (When Data Entered)

(Block 20 continued)

The first three models generated were analyzed by NASTRAN, and the third and fourth models were analyzed by CORTES/SA, resulting in a total of five finite element analyses. Flexibility factors and normalized principal stresses were then compared to experimentally obtained results. One of the four models investigated was generated from actual measured geometry using GPRIME, a geometric and finite element modeling system developed at DTNSRDC. The other three models were generated from an idealized tee using the data generator contained in CORTES/SA. The generation by GPRIME of the finite element model from actual geometry was more difficult and expensive than the generation by CORTES/SA of an idealized model of the tee. In addition, the idealized model proved to be adequate when analyzed by NASTRAN.

Results from the NASTRAN analyses were in good agreement with the experimental results for all loadings except internal pressure. The CORTES/SA analyses of the idealized tees gave good results for the internal pressure loading but poorer results for out-of-plane bending moments or for forces resulting in out-of-plane bending. Two of the basic load cases in CORTES/SA were found to contain errors that could not be easily corrected. A cost comparison of NASTRAN and CORTES/SA analyses showed that, for identical meshes, NASTRAN was less expensive to run.

Overall, considering modeling effort, cost, and accuracy, it is recommended that tees be analyzed by NASTRAN using an idealized mesh generated by CORTES/SA.

UNCLASSIFIED

SECURITY CLASSIFICATION OF THIS PAGE (When Data Entered)

## TABLE OF CONTENTS

	Page
LIST OF FIGURES.....	iii
LIST OF TABLES.....	v
ABSTRACT.....	1
ADMINISTRATIVE INFORMATION.....	2
BACKGROUND.....	2
STATEMENT OF THE PROBLEM.....	3
ANALYSES PERFORMED.....	4
STRESS RESULTS.....	6
FLEXIBILITY FACTORS.....	7
DISCUSSION OF RESULTS AND CONCLUSIONS.....	10
ACKNOWLEDGMENTS.....	11
REFERENCES.....	41

## LIST OF FIGURES

1 - Schematic View of Applied Loads for Test Tee.....	17
2 - Location of Strain Gage Rows on Test Tee.....	18
3 - Finite Element Model of Tee Using Actual Geometry; Mesh 1.....	19
4 - Finite Element Model of Tee Using Idealized Geometry; Mesh 2.....	20
5 - Finite Element Model of Tee Using Idealized Geometry; Mesh 3.....	21
6 - Finite Element Model of Tee Using Idealized Geometry; Mesh 4.....	22
7 - Geometry Input Parameters for Idealized Mesh Generation.....	23
8 - Normalized Stress Intensity for Load Case 1 (M3X), Row 1, Major Principal Stress on Outer Surface.....	24

	Page
9 - Normalized Stress Intensity for Load Case 2 (M3Y), Row 1, Major Principal Stress on Outer Surface.....	25
10 - Normalized Stress Intensity for Load Case 3 (M3Z), Row 6, Minor Principal Stress on Outer Surface.....	26
11 - Normalized Stress Intensity for Load Case 5 (F3Y), Row 1, Major Principal Stress on Outer Surface.....	27
12 - Normalized Stress Intensity for Load Case 6 (F3Z), Row 1, Major Principal Stress on Outer Surface.....	28
13 - Normalized Stress Intensity for Load Case 7 (M2X), Row 1, Major Principal Stress on Outer Surface.....	29
14 - Normalized Stress Intensity for Load Case 7 (M2X), Row 1, Minor Principal Stress on Outer Surface.....	30
15 - Normalized Stress Intensity for Load Case 8 (M2Y), Row 1, Minor Principal Stress on Inner Surface.....	31
16 - Normalized Stress Intensity for Load Case 9 (M2Z), Row 1, Minor Principal Stress on Inner Surface.....	32
17 - Normalized Stress Intensity for Load Case 10 (F2X), Row 1, Major Principal Stress on Inner Surface.....	33
18 - Normalized Stress Intensity for Load Case 11 (F2Y), Row 1, Minor Principal Stress on Inner Surface.....	34
19 - Normalized Stress Intensity for Load Case 12 (F2Z), Row 1, Major Principal Stress on Inner Surface.....	35
20 - Normalized Stress Intensity for Load Case 13 (P), Row 6, Major Principal Stress on Inner Surface.....	36
21 - Superimposed Plots of Undeformed and Deformed Tee Model Due to In-Plane Bending Moment on the Run (M2Z).....	37
22 - Superimposed Plots of Undeformed and Deformed Tee Model Due to Out-of-Plane Bending Moment on the Run (M2Y)....	38
23 - Superimposed Plots of Undeformed and Deformed Tee Model Due to Torsional Moment on the Run (M2X).....	39



## LIST OF TABLES

	Page
1 - Summary of Applied and Normalized Loads.....	12
2 - Comparison of Finite Element Analysis: NASTRAN vs. CORTES.....	13
3 - Input Parameters Used for Generation of Idealized Geometry.....	14
4 - Summary of Nominal Rotations Used to Compute Flexibility Factors.....	15
5 - Comparison of Flexibility Factors of Experimental Results to NASTRAN Results.....	16

## ABSTRACT

Finite element analyses were performed for a 24" x 24" x 10" schedule 40 carbon steel piping tee subjected to five orthogonal forces, six orthogonal moments, and internal pressure. The NASTRAN and CORTES/SA computer programs were used to compute displacements and normalized principal stresses for four finite element models. (CORTES/SA is a special purpose finite element analysis program for tee joints developed at the University of California at Berkeley.) The first three models generated were analyzed by NASTRAN, and the third and fourth models were analyzed by CORTES/SA, resulting in a total of five finite element analyses. Flexibility factors and normalized principal stresses were then compared to experimentally obtained results. One of the four models investigated was generated from actual measured geometry using GPRIME, a geometric and finite element modeling system developed at DTNSRDC. The other three models were generated from an idealized tee using the data generator contained in CORTES/SA. The generation by GPRIME of the finite element model from actual geometry was more difficult and expensive than the generation by CORTES/SA of an idealized model of the tee. In addition, the idealized model proved to be adequate when analyzed by NASTRAN.

Results from the NASTRAN analyses were in good agreement with the experimental results for all loadings except internal pressure. The CORTES/SA analyses of the idealized tees gave good results for the internal pressure loading but poorer results for out-of-plane bending moments or for forces resulting in out-of-plane bending. Two of the basic load cases in CORTES/SA were found to contain errors that could not be easily corrected. A cost comparison of NASTRAN and CORTES/SA analyses showed that, for identical meshes, NASTRAN was less expensive to run.

Overall, considering modeling effort, cost, and accuracy, it is recommended that tees be analyzed by NASTRAN using an idealized mesh generated by CORTES/SA.

## ADMINISTRATIVE INFORMATION

This work was sponsored by the Naval Sea Systems Command in Program Element/Task Area 63561N/S0348001, Task 21302, Work Unit 1-2740-163. Naval Sea Systems Command cognizant program manager is Dr. F. Ventriglio (NAVSEA 05R).

## BACKGROUND

The designer of a piping system requires a knowledge of the deflections and stresses caused throughout the system by anticipated service loads. Of particular interest are critical components such as elbows and tees. Although the finite element method is mature enough in its development to be expected to predict the required information reliably, it has so far had little application to piping components.

The purpose of this study, therefore, is to assess the effectiveness of the finite element method (FEM) in predicting flexibility factors and stresses in piping tees subjected to force, moment, and pressure loadings. A similar study,<sup>1\*</sup> performed recently for piping elbows, indicated that very good agreement could be expected between FEM analysis and experiment. Tees, although conceptually no more difficult to analyze than elbows, are considerably more complicated geometrically. A reducing tee, for example, has in the crotch region a fillet with a variable radius of curvature as well as variable thickness. Moreover, the adjacent straight sections may not be cylindrical. Thus, geometrical idealizations of tees, although plausible, may be incorrect.

The finite element analyses described here involve idealized models as well as a model based on actual measured geometry. Two computer programs were used for the analyses: NASTRAN, a widely-used general purpose finite element structural analysis program, and CORTES/SA,<sup>2</sup> a special purpose finite element tee analysis program written at the University of California at Berkeley under the sponsorship of the Oak

---

\* A complete listing of references is given on page 41.

Ridge National Laboratory.\* This series of analyses was designed to provide information on the sensitivity of the results to various mesh densities as well as on the adequacy of the assumed idealizations.

In this report, the program CORTES/SA will be referred to by the abbreviated name "CORTES".

#### STATEMENT OF THE PROBLEM

Combustion Engineering, Inc., performed an experimental stress analysis<sup>3</sup> on an ANSI B16.9 carbon steel<sup>†</sup> tee designated T-12. Pipe extensions were welded to the branch and run ends of the tee, and the resulting assembly was placed in a load frame. One of the run ends was built in to represent a fixed end, and the other run end and the branch end were used to apply six orthogonal moments and five orthogonal forces. Internal pressure was also applied. Table 1 and Figure 1 summarize the applied loads. Note that load case 4 (F3X) was not tested because of strength limitations of the load frame. Stress data for all twelve load cases were gathered from strain gages fixed on specific rows on the tee (Figure 2) and were plotted against normalized surface distance.

The tee analyzed was a reducing tee with a 24-inch-diameter run end and a 10.75-inch-diameter branch. Loads to the run were applied at the free end of the run pipe extension, 173 inches from the branch-run intersection (Figure 1). Loads to the branch were applied at the end of the branch pipe extension, 77 inches from the branch-run intersection. The run pipe extension consisted of 24-inch-diameter schedule 40 (0.687-inch nominal wall thickness) carbon steel piping. The branch pipe extension consisted of 10.75-inch-diameter schedule 40 (0.365-inch nominal wall thickness) carbon steel piping.

---

\* The CORTES package of computer programs is distributed as program number 759 by the National Energy Software Center (NESC), Argonne National Laboratory, 9700 S. Cass Avenue, Argonne, Illinois 60439.

<sup>†</sup> The material properties for carbon steel are  $E = 30 \times 10^6$  psi (Young's modulus) and  $\nu = 0.3$  (Poisson's ratio).

The finite element analyses of the tee simulated these loading conditions so that stresses at selected locations could be compared to the experimental results. For most load cases, the strain gage rows (Figure 2) selected for comparison were those on which the peak stresses occurred.

#### ANALYSES PERFORMED

NASTRAN analyses were performed for the first three models generated, and CORTES analyses were performed for the third and fourth models. These five finite element analyses are summarized in Table 2. In the abbreviations N1, N2, N3, C3, and C4 used to identify the analyses, the first character (N or C) indicates the analysis program used (NASTRAN or CORTES), and the second character indicates the mesh used. The four meshes are plotted in Figures 3 through 6. In general, a higher mesh number corresponds to a finer mesh, either overall or in selected key regions of the tee.

The NASTRAN analysis of Mesh 1 was the only analysis performed for a model generated from actual measured geometry. The remaining analyses were performed either by NASTRAN or by CORTES on meshes generated by CORTES assuming an idealized geometry. In all cases only one-fourth of the actual tee was modeled due to symmetry. The -X, +Y, -Z quadrant was modeled, where the X-axis coincides with the run centerline, and the positive Y-axis coincides with the branch centerline, as shown in Figure 1.

For the NASTRAN analyses, the tee, including pipe extensions, was modeled with plate (NASTRAN QUAD2) elements. A QUAD2 element is a quadrilateral bending and membrane plate with four nodes, one at each corner. Beam (BAR) elements were arranged in a spoke formation radiating from an imaginary point in the center of the cross section at the ends of the tee branch and run to facilitate the calculation of the average rotation of these cross sections. Rigid (RIGD1) elements were defined at the ends of the pipe extensions for use in load application. The loads were applied to a point in the center of the rigid cross section at the ends of the pipe extensions.

In the CORTES analyses, the tee and pipe extensions were modeled using an 8-node hexahedral element. This element, designated ZIB8R9, is a modification of the standard Zienkiewicz-Irons isoparametric element and, according to Gantayat and Powell,<sup>2</sup> has bending properties superior to those of the unmodified isoparametric element. The loads are applied at the ends of the pipe extensions to which are added stiff flanges modeled by elements with an artificially large modulus of elasticity. The loads are decomposed into statically equivalent forces and then uniformly distributed over the elements at the end of the pipe extensions. (This decomposition was unnecessary with the rigid flange approach taken with NASTRAN.)

When a mesh was generated by CORTES for analysis by NASTRAN, the CORTES ZIB8R9 elements were replaced with NASTRAN plate (QUAD2) elements, except for the elements in the stiff flanges at the ends of the pipe extensions, which were replaced with NASTRAN rigid (RIGD1) elements. Loading then proceeded as described earlier for the NASTRAN models.

Mesh 1 was modeled from actual geometry as specified in the Combustion Engineering, Inc., report,<sup>3</sup> which tabulated coordinates of points on the outer surface of the tee and thicknesses at these points. From these digitized data, a general B-spline surface was fitted through the supplied points using the geometric and finite element modeling processor GPRIME.<sup>4,5</sup> Once this geometric model was defined, GPRIME was used to generate a finite element mesh which included the effects of variable thicknesses.

Meshes 2 through 4 were modeled as idealized tee joints using the automatic mesh generation routine in CORTES. The tee joint is idealized (Figure 7) by shallow cones representing the branch and run portions of the tee, connected to each other through a transition fillet. Circular pipe extensions connected to the ends of the shallow cones represent the branch and run pipe extensions. The parameters required to define the geometry of the idealized tee joint, as well as the actual values used for T-12, are listed in Table 3. See also Figure 7.

Of the three idealized meshes, Mesh 2 is the coarsest and is approximately equivalent to Mesh 1 in number of nodes, elements, and

degrees of freedom. Mesh 3 is similar to Mesh 2 except that it has more elements in the run area of the tee, resulting in approximately 25% more elements. Mesh 4 is the finest mesh overall, having approximately 20% more elements than Mesh 3.

In all four meshes, the aspect ratios of the elements within the branch and run areas of the tee were kept as close as possible to unity. In the pipe extension, the mesh was allowed to expand outwards until elements approached an aspect ratio of approximately 2 to 1.

### STRESS RESULTS

The results of primary interest are normalized principal stress values for elements in particular locations on the tee. The peak normalized principal stress was plotted against surface distance ratio for each load case and compared to the experimental results obtained by Combustion Engineering, Inc.<sup>3</sup>

The tee analyzed by Combustion Engineering, Inc., was heavily instrumented, both internally and externally, with strain gages in two of the four quadrants. The gages in each quadrant were arranged in six rows as shown in Figure 2. Since the peak stresses for most load cases occurred on row 1 or row 6, analytical and experimental results were compared for these rows only. Row 1, the first row of each quadrant, is located in the Y-Z plane; row 6 is located in the X-Y plane.

For each load case, the analytical results for principal stresses were normalized by a stress calculated from beam theory, as indicated in Table 1. The normalized principal stresses were then plotted against the surface distance ratios of the elements lying on row 1 and row 6. The surface distance ratio of a gage in a particular row on the run is computed by determining the surface distance of the gage from the crotch line, and dividing it by the distance of the gage on the same row of the run most distant from the crotch line. Surface distance ratios of gages on the branch are computed in the same way. The surface distance ratio of the most distant gage in a row on the run is -1, and the surface distance ratio of the most distant gage in a row on the branch is +1. From the known surface distance ratios and coordinates of the gages on

rows 1 and 6 and the known coordinates of the centroids of the elements corresponding to gages on rows 1 and 6, the surface distance ratios of the elements can be determined.

To avoid making the 96 possible plots resulting from the many combinations of internal and external gages, maximum and minimum principal stresses, two rows (1 and 6), and twelve load cases, usually the only curve plotted for a load case was the one containing the peak value of stress.

The stress plots for the various load cases are shown in Figures 8 through 20. All finite element curves are smoothed slightly by fitting B-spline curves<sup>6,7</sup> through the computed values, which are located at element centroids for the NASTRAN results and at grid points for the CORTES results.

Figures 21 through 23 show plots of deformed tees superimposed on undeformed models for several typical load cases. Recall that, due to symmetry, only one-fourth of the tee was modeled. This required treating the reactions at the fixed support as applied loads. As a result, the deformations shown in Figures 21 through 23 exhibit either symmetry or antisymmetry with respect to the Y-Z plane. This "redefinition" of the problem is equivalent to superimposing a rigid body translation and rotation on the actual deformations, so that stresses and relative displacements are unaffected.

#### FLEXIBILITY FACTORS

Two ambiguities were encountered in comparing computed flexibility factors with experimental results obtained by Combustion Engineering, Inc. These ambiguities involved the definition of flexibility factors and the way in which the rotation of branch or run end cross sections was measured. Combustion Engineering, Inc., defined the flexibility factors as

$$k = \frac{\theta_{\text{meas}} - \theta_{\text{corr}}}{\theta_{\text{nom}}} \quad (1)$$

where

$\theta_{\text{meas}}$  = measured rotation at an intermediate location on the pipe extension



$\theta_{\text{corr}}$  = rotation correction computed by simple beam theory for the length of pipe between the tee weld line and the location at which the rotation is actually measured

$\theta_{\text{nom}}$  = nominal rotation computed by simple beam theory for the distance between the tee weld lines where

$$\theta_{\text{nom}} = \frac{ML}{EI} \quad (\text{for bending moments}) \quad (2)$$

$$\theta_{\text{nom}} = \frac{TL}{JG} \quad (\text{for torsional moments}) \quad (3)$$

$$\theta_{\text{nom}} = \frac{PL^2}{2EI} \quad (\text{for point loads}) \quad (4)$$

Note that a nominal rotation may consist of rotations due to several forces. The nominal rotation for load case 12 (F2Z), for example, consists of a rotation due to the force load and a rotation due to a moment load, where the magnitude of the moment is equal to the product of the applied force and the length of the run pipe extension. Table 4 summarizes the nominal rotations used for calculation of flexibility factors for the various load cases.

Since Combustion Engineering, Inc., could not measure the actual rotations at the branch and run end cross sections, measurements were made at other locations on the pipe extensions and then corrected to the branch and run ends using simple beam theory. On the other hand, the NASTRAN analyses used very flexible beam elements radiating from an imaginary point in the center of the branch and run end cross sections to the points on the circumference of the branch and run ends. Giving the beam elements geometric properties (area and moment of inertia) proportional to the angles between adjacent beam elements allows an approximate average rotation for the cross sections to be easily obtained for the imaginary center point. At the branch end, the nodes on the circumference of the cross section were uniformly spaced, resulting in beam elements with equal geometric properties. At the run end, the nodes were not uniformly spaced, which complicated the assignment of geometric properties. However, because plane sections do not, under loading, remain plane, there is no single rotation for a section, so that different methods for

computing rotations will yield different results.

For the computation of flexibility factors from the NASTRAN results, the relation

$$k = \frac{\theta_{ab}}{\theta_{nom}}$$

was used, where

$\theta_{ab}$  = computed relative rotation of end "a" with respect to end "b"

$\theta_{nom}$  = nominal rotation computed by beam theory for the rotation of end "a" with respect to end "b"

Flexibility factors were computed for the free branch and run ends with respect to the fixed run end for each load case except for F2X (an axial load on the run) and internal pressure, neither of which causes any significant rotation. For example, the flexibility factor for a rotation about the X-axis of the branch end with respect to the fixed run end is denoted by  $k_{X31}$ , where the X in the subscript represents the axis of rotation, the 3 represents the branch end, and the 1 represents the fixed run end. For each load case, flexibility factors for each cross section were computed.

Table 5 compares the flexibility factors computed from the three NASTRAN analyses to the experimental values. The computed flexibility factors compare reasonably well for most load cases, an exception being  $k_{Z21}$  for load case 5 (F3Y) of N2. Combustion Engineering, Inc., did not compute flexibility factors for this load case because the stresses and deflections were considered too small to give reliable answers. The displacements computed in the three NASTRAN analyses for load case 5, however, did not appear to be significantly smaller than those of the other load cases, although the run end of the tee did warp severely in all three analyses. Since the distortions in all three analyses were similar, it appears to have been due to chance that the flexibility factors for N1 and N3 were not also negative for this load case. This implies that any method used to compute a single rotation of the run end is inadequate for severely distorted cross sections. Moreover, the usefulness of a flexibility factor when severe cross-sectional distortion occurs is questionable.

In general, a negative flexibility factor, whether arising from experiment or analysis, is physically impossible, since such a factor implies a rotation in a direction opposite to that of the applied moment. Negative values can arise experimentally whenever rotations measured at one location have to be "corrected" (using beam theory) to yield rotations elsewhere. Negative values can result from a finite element analysis whenever severe cross-sectional distortion occurs, in which case the usefulness of an "average" rotation of the cross-section is in doubt.

#### DISCUSSION OF RESULTS AND CONCLUSIONS

The three NASTRAN analyses of the tee joint were generally in very good agreement with the experimental results and accurately predicted peak stresses for most loadings except load cases 3 (M3Z) and 13 (pressure). Also, as expected, the agreement with the experimental results improved with finer meshes. In general, the two CORTES analyses were slightly less accurate than the NASTRAN analyses except for load case 13 (pressure). We are unable to explain this behavior. While the CORTES results for pressure loading were significantly better than NASTRAN's, the results for load cases 1 (M3X), 8 (M2Y), 10 (F2X), and 12 (F2Z) were worse. Note that most of these load cases involve either out-of-plane bending moments or forces resulting in out-of-plane bending. The CORTES analyses of load cases 6 (F3Z) and 7 (M2X) were also found to contain errors in formulation and coding which could not be easily corrected.

The preparation of the NASTRAN model of mesh 1 (called N1) was the most time-consuming and expensive of all the models, since this mesh was generated from actual geometry. Although the N1 calculations for all load cases except pressure (Figure 20) are in very good agreement with the experimental results, they are not significantly better than those obtained from the other analyses, so the extra effort is not justified.

In a comparison of NASTRAN and CORTES analyses of an identical mesh (Mesh 3), the NASTRAN results (N3) were more consistent and predicted peak stresses more accurately than CORTES for ten of the twelve load cases. Only for M3Z (Fig. 10) and pressure (Fig. 20) did C3 do better

than N3. Although N3 was less expensive than C3 in computer costs, it required slightly more time for input preparation.

Since N3 was in generally better agreement with experimental results than C3, a coarser mesh (Mesh 2) was also analyzed by NASTRAN (N2) and compared with C3. In all but three of the load cases, M3Z (Fig. 10), F3Y (Fig. 11), and pressure (Fig. 20), N2 was again in better agreement with experimental results than C3. Computer costs from N2 were significantly less than those for C3, as indicated in Table 2.

In an effort to obtain better results from CORTES, a much finer mesh (Mesh 4) was generated and analyzed, so that the results could be compared with N3. This time, overall performance was about equal for the two analyses, although C4 achieved better results than N3 for M3Z (Fig. 10), F3Y (Fig. 11), M2Z (Fig. 16), F2Y (Fig. 18), and pressure (Fig. 20).

In conclusion, it is apparent that GPRIME, although well-suited in general to the generation of tee meshes based on actual geometry, is more difficult and time-consuming to use than the special purpose idealized tee generator contained in CORTES. Models based on actual geometry also require geometric data that would probably not be generally available to the analyst. For these reasons, CORTES generation of a finite element model based on idealized geometry appears to be acceptable. However, if an analyst is interested in an F3Z or an M2X loading, CORTES should not be used as the analyzer because the program currently contains errors in the coding of these two load cases. Also, as shown by the comparison of N3 with C4, CORTES requires a mesh about 20% finer to obtain results as accurate as NASTRAN.

Overall, considering modeling effort, cost, and accuracy, it is recommended that tees be analyzed by NASTRAN using an idealized mesh generated by CORTES/SA.

#### ACKNOWLEDGMENTS

The authors acknowledge with pleasure the fruitful discussions held with Mr. L. Kaldor and Dr. Y.P. Lu (Machinery Stress Analysis Branch, Code 2744), as well as the GPRIME consultation provided by Mr. J.M. McKee (Numerical Structural Mechanics Branch, Code 1844).

TABLE 1 - SUMMARY OF APPLIED AND NORMALIZED LOADS

Load Case	Applied Load	Nominal Stress	Normalized Load
1. M3X	4.29E5 in-lb	$\frac{M3X}{Z_b}$	29.91
2. M3Y	-6.03E5 in-lb	$\frac{M3Y}{Z_b}$	29.91
3. M3Z	5.98E5 in-lb	$\frac{M3Z}{Z_b}$	29.91
5. F3Y	4.0E4 lb	$\frac{F3Y}{A_b}$	11.91
6. F3Z	5.58E3 lb	$\frac{77F3Z}{Z_b}$	3.884E-1
7. M2X	4.9E6 in-lb	$\frac{M2X}{Z_r}$	285.0
8. M2Y	-7.54E6 in-lb	$\frac{M2Y}{Z_r}$	285.0
9. M2Z	3.40E6 in-lb	$\frac{M2Z}{Z_r}$	285.0
10. F2X	-6.28E5 lb	$\frac{F2X}{A_r}$	50.3
11. F2Y	2.01E4 lb	$\frac{173F2Y}{Z_r}$	1.6474
12. F2Z	2.46E4 lb	$\frac{173F2Z}{Z_r}$	1.6474
13. P	600 psi	$\left( \frac{P D_0}{2t} \right)_r$	5.725E-2

**Notes:**

1. Load case 4 (F3X) was not tested.
2. The "normalized load" is computed by dividing the experimentally applied load (column 2) by the nominal stress (column 3).
3. Subscripts "r" and "b" above denote "run" and "branch", respectively.

**TABLE 2 - COMPARISON OF FINITE ELEMENT ANALYSES:  
NASTRAN vs. CORTES**

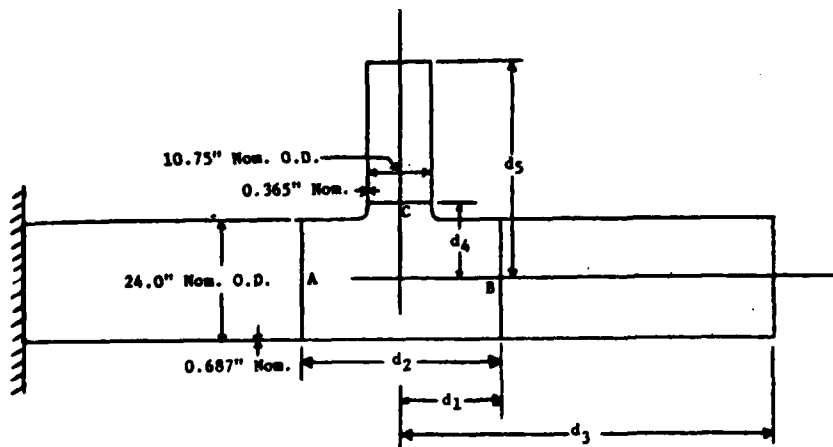
	N1	N2	N3	C3	C4
NASTRAN or CORTES Analysis	NASTRAN	NASTRAN	NASTRAN	CORTES	CORTES
Idealized or Actual Geometry	Actual	Idealized	Idealized	Idealized	Idealized
Number of Elements	432	420	525	549	626
Number of Nodes	484	473	583	609	689
Number of Degrees of Freedom	2525	2462	3047	3458	3958
Total CP Seconds (CDC 6400)	2213	2200	3135	3310	4748
Cost	\$228	\$226	\$335	\$421	\$605

TABLE 3 - INPUT PARAMETERS USED FOR GENERATION  
OF IDEALIZED GEOMETRY

Diameter of branch end of tee	10.75 in.
Diameter of run end of tee	24.0 in.
Diameter of branch pipe extension	10.75 in.
Diameter of run pipe extension	24.0 in.
Length of branch from run centerline	15.138 in.
Length of run from branch centerline	17.005 in.
Total length of branch and branch pipe extension from run centerline	36.637 in.
Total length of run and run pipe extension from branch centerline	65.005 in.
Cone angle of branch ( $\alpha$ )	1.823276 deg.
Cone angle of run ( $\beta$ )	2.956345 deg.
Radius of curvature of transition fillet in Y-Z plane (point A)	3.655134 in.
Radius of curvature of transition fillet in X-Y plane (point B)	2.085379 in.
Thickness at control node 0	1.09954 in.
Thickness at control node 1	1.09256 in.
Thickness at control node 2	0.365 in.
Thickness at control node 3	0.365 in.
Thickness at control node 4	0.365 in.
Thickness at control node 5	0.95769 in.
Thickness at control node 6	0.970 in.
Thickness at control node 7	0.97867 in.
Thickness at control node 8	0.687 in.
Thickness at control node 9	0.687 in.
Thickness at control node 10	0.687 in.

TABLE 4 - SUMMARY OF NOMINAL ROTATIONS USED TO COMPUTE FLEXIBILITY FACTORS

Load Case	$\theta_{\text{nom AB}}$	$\theta_{\text{nom AC}}$
1. M3X	$(\text{M3X})(d_1)/J_r G$	$(\text{M3X})(d_4)/EI_b + (\text{M3X})(d_1)/J_r G$
2. M3Y	$(\text{M3Y})(d_1)/EI_r$	$(\text{M3Y})(d_4)/J_b G + (\text{M3Y})(d_1)/EI_r$
3. M3Z	$(\text{M3Z})(d_1)/EI_r$	$(\text{M3Z})(d_4)/EI_b + (\text{M3Z})(d_1)/EI_r$
5. F3Y	$(\text{F3Y})(d_1)^2/2EI_r$	$(\text{F3Y})(d_1)^2/2EI_r$
6. F3Z	$(d_5 \text{F3Z})(d_1)/J_r G$	$(\text{F3Z})(d_4)^2/2EI_b + (d_5 - d_4) \text{F3Z}(d_4)/EI_b + (d_5 \text{F3Z})(d_1)/J_r G$
7. M2X	$(\text{M2X})(d_2)/J_r G$	$(\text{M2X})(d_1)/J_r G$
8. M2Y	$(\text{M2Y})(d_2)/EI_r$	$(\text{M2Y})(d_1)/EI_r$
9. M2Z	$(\text{M2Z})(d_2)/EI_r$	$(\text{M2Z})(d_1)/EI_r$
11. F2Y	$(\text{F2Y})(d_2)^2/2EI_r + (d_3 - d_1) \text{F2Y}(d_2)/EI_r$	$(d_3 \text{F2Y})(d_1)/EI_r + (\text{F2Y})(d_1)^2/2EI_r$
12. F2Z	$(\text{F2Z})(d_2)^2/2EI_r + (d_3 - d_1) \text{F2Z}(d_2)/EI_r$	$(d_3 \text{F2Z})(d_1)/EI_r + (\text{F2Z})(d_1)^2/2EI_r$



$d_1 = 17.005 \text{ in.}$   
 $d_2 = 34.01 \text{ in.}$   
 $d_3 = 173.0 \text{ in.}$   
 $d_4 = 15.138 \text{ in.}$   
 $d_5 = 77.0 \text{ in.}$

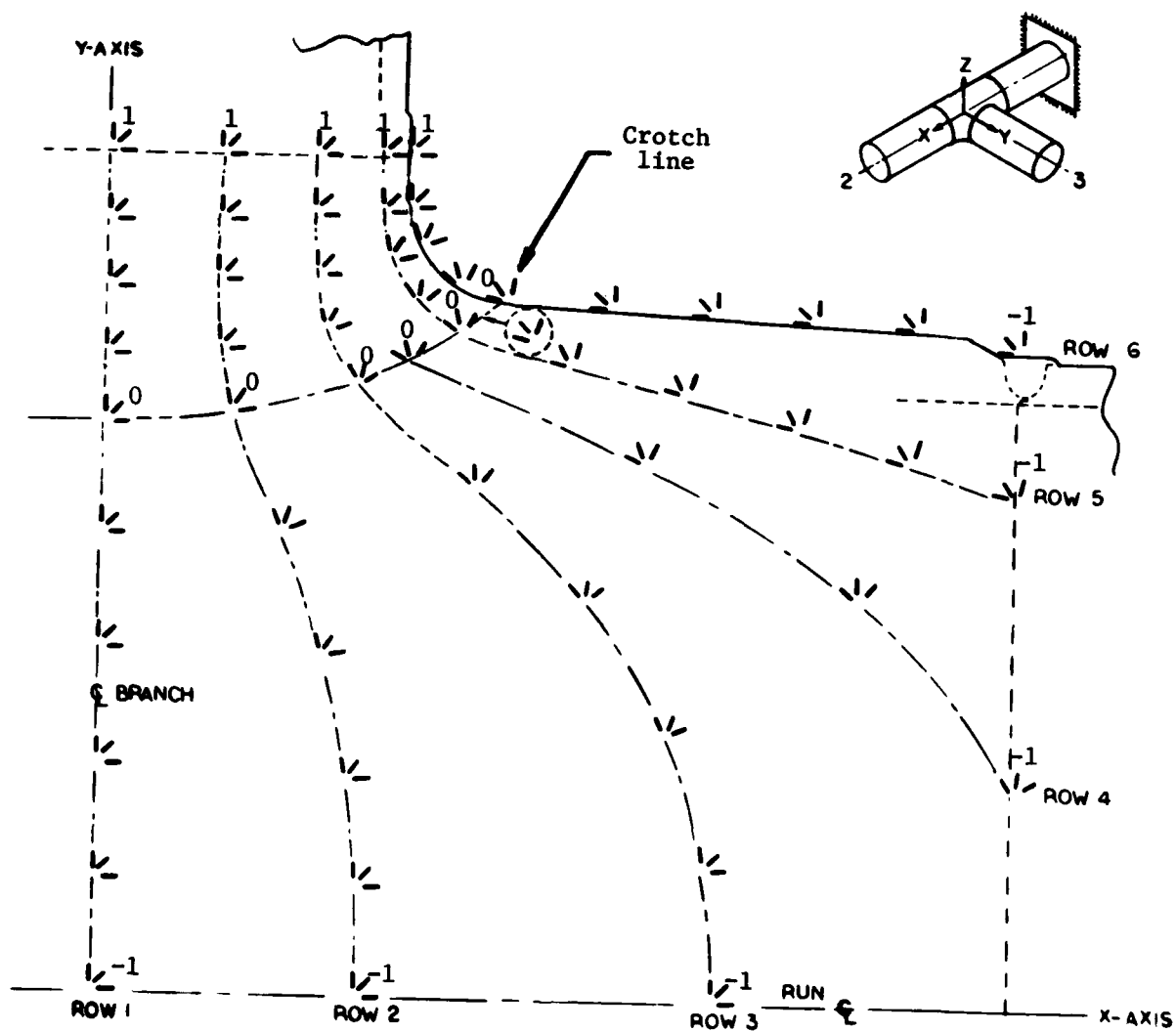


**TABLE 5 - COMPARISON OF FLEXIBILITY FACTORS OF  
EXPERIMENTAL RESULTS TO NASTRAN RESULTS**

Load Case	k Subscript	Experiment	N1	N2	N3
1. M3X	X21	-0.8	0.82	1.00	0.85
	X31	1.8	2.40	4.00	2.73
2. M3Y	Y21	0.5	0.72	0.76	0.77
	Y31	-0.3	0.32	0.33	0.32
3. M3Z	Z21	0.5	0.73	1.03	0.93
	Z31	0.9	0.90	0.85	0.84
5. F3Y	Z21		1.22	-1.35	1.53
	Z31		1.97	0.51	2.08
6. F3Z	X21		0.85	1.09	0.88
	X31	1.8	2.97	4.94	3.40
7. M2X	X21	-0.4	0.82	1.00	0.85
	X31	-0.5	0.82	1.00	0.85
8. M2Y	Y21	0.7	0.72	0.76	0.77
	Y31	0.6	0.72	0.76	0.77
9. M2Z	Z21	0.9	0.73	1.01	0.93
	Z31	0.8	0.73	1.01	0.93
11. F2Y	Z21	0.8	0.73	1.01	0.93
	Z31	0.8	0.83	1.08	1.01
12. F2Z	Y21	0.7	0.72	0.76	0.77
	Y31	0.7	0.91	0.89	0.94

The diagram illustrates a beam-column joint under a specific load condition. A horizontal beam is shown with a vertical column intersecting it. The beam is supported by a fixed base on the left. Three planes are identified: Plane 1 at the base, Plane 2 at the joint, and Plane 3 at the end of the beam. Internal forces are labeled at these planes: at Plane 1, M1Z, F1Z, and F1Y; at Plane 2, M2Z, F2Z, F2Y, M2X, F2X, and F2Y; and at Plane 3, M3Z, F3Z, F3Y, M3X, F3X, and F3Y. A coordinate system (X, Y, Z) is shown at the joint, with Z pointing up, Y pointing right, and X pointing out of the page. The beam is labeled 'P L.C. 13'.

**Figure 1 - Schematic View of Applied Loads for Test Tee**



Source: Figure 4, Ref. 3

Figure 2 - Location of Strain Gage Rows on Test Tee

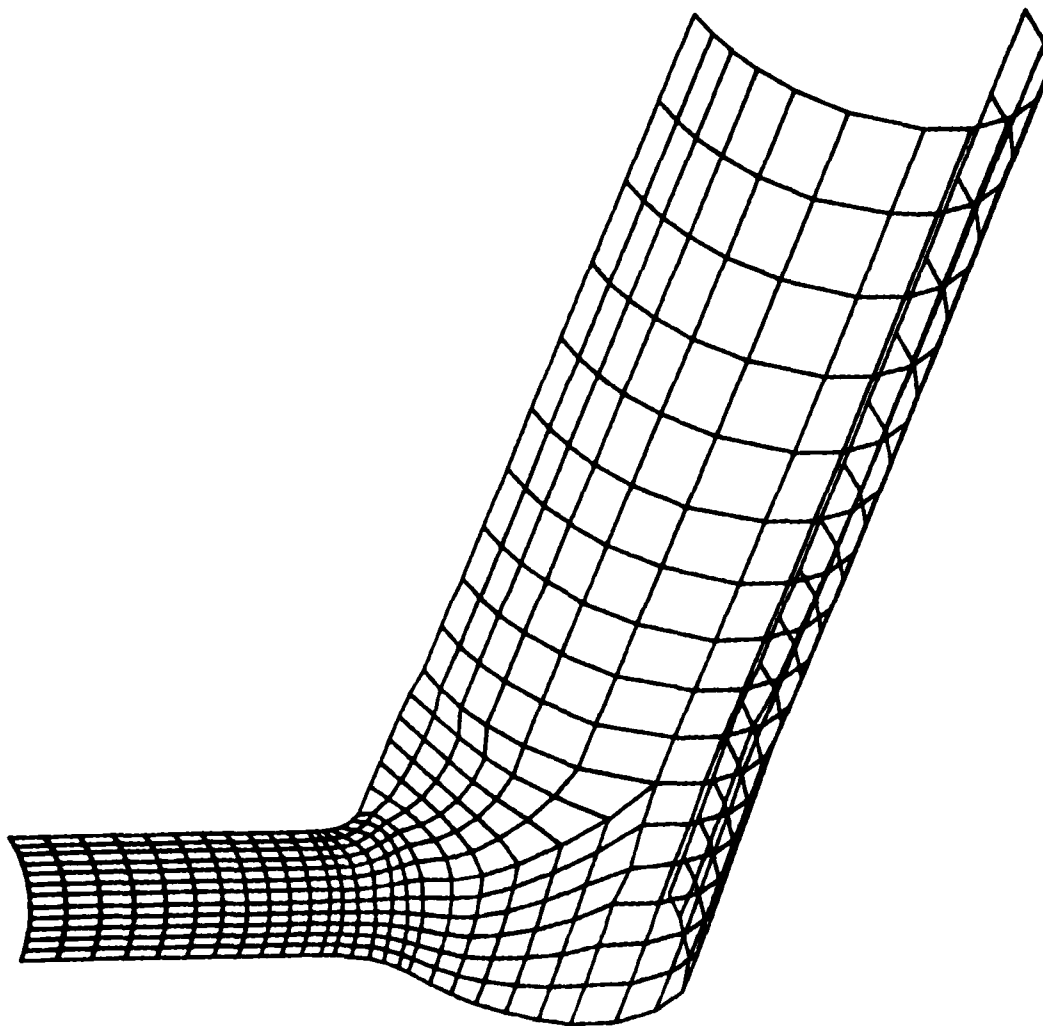


Figure 3 - Finite Element Model of Tee Using Actual Geometry; Mesh 1

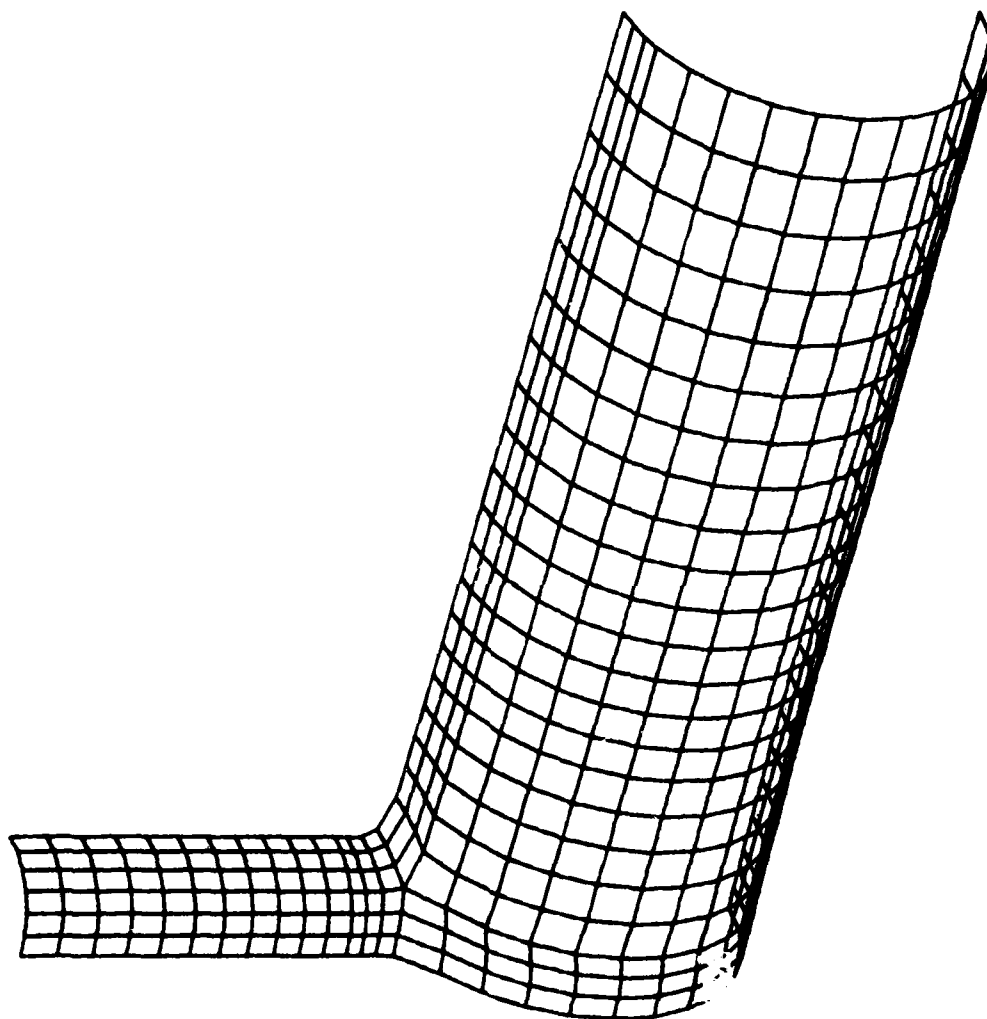


Figure 4 - Finite Element Model of Tee Using Idealized Geometry; Mesh 2

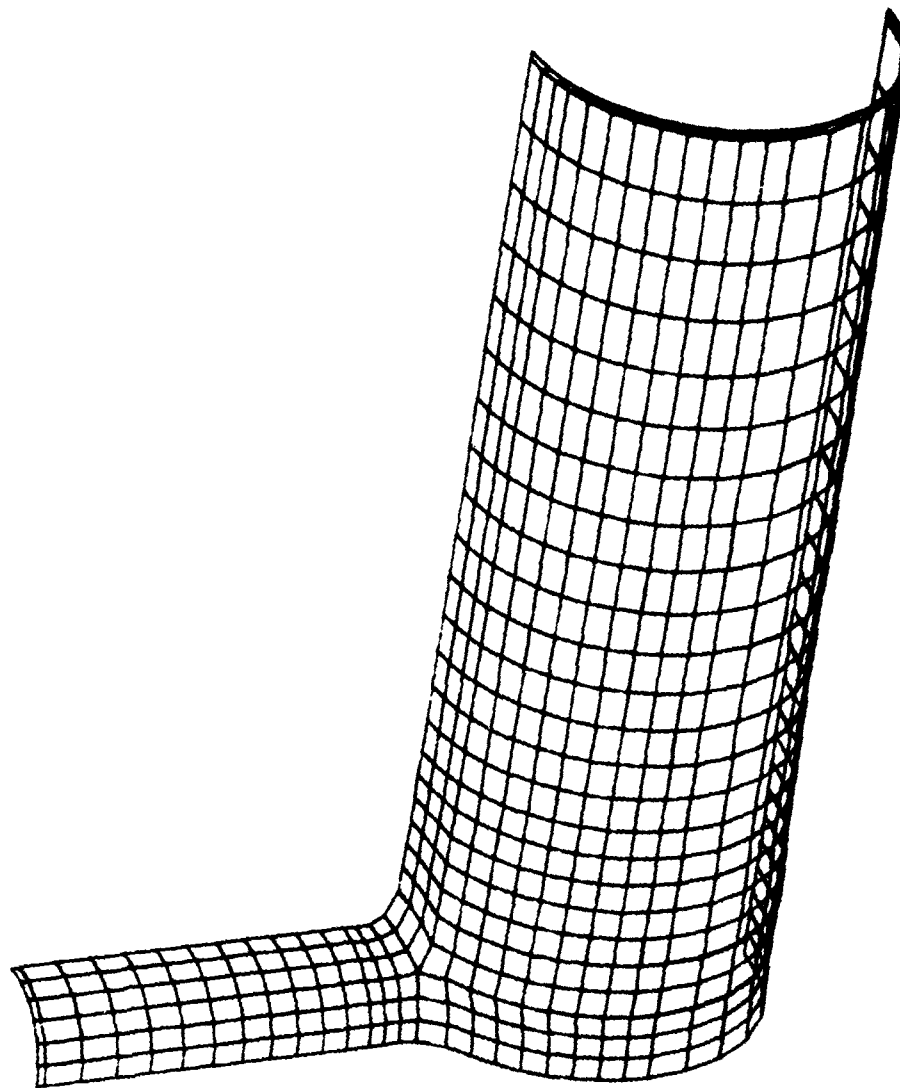


Figure 5 - Finite Element Model of Tee Using Idealized Geometry; Mesh 3

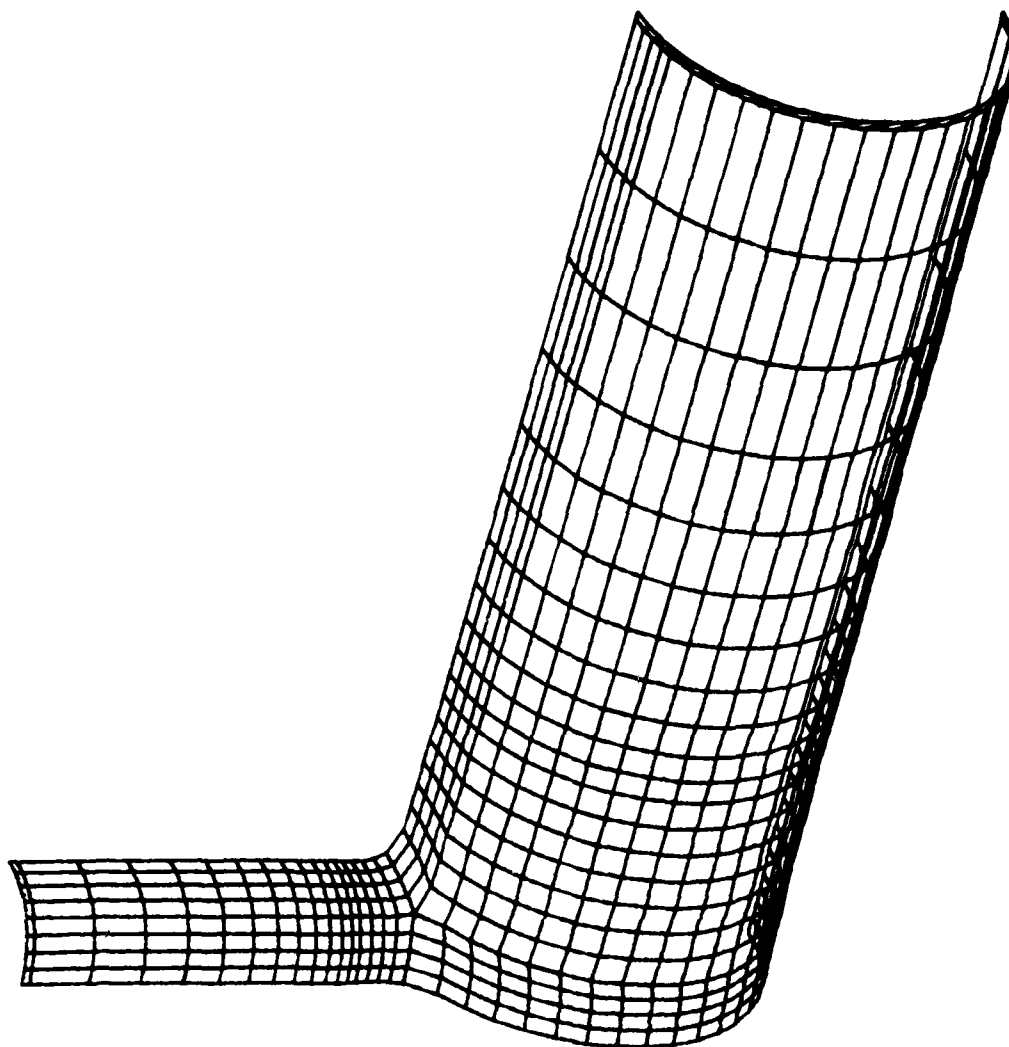
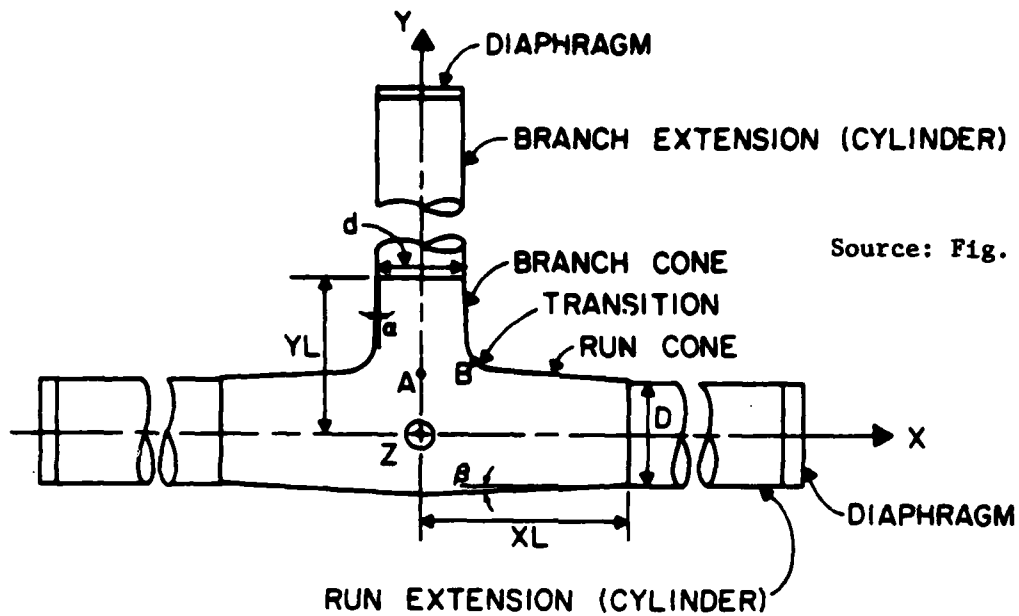
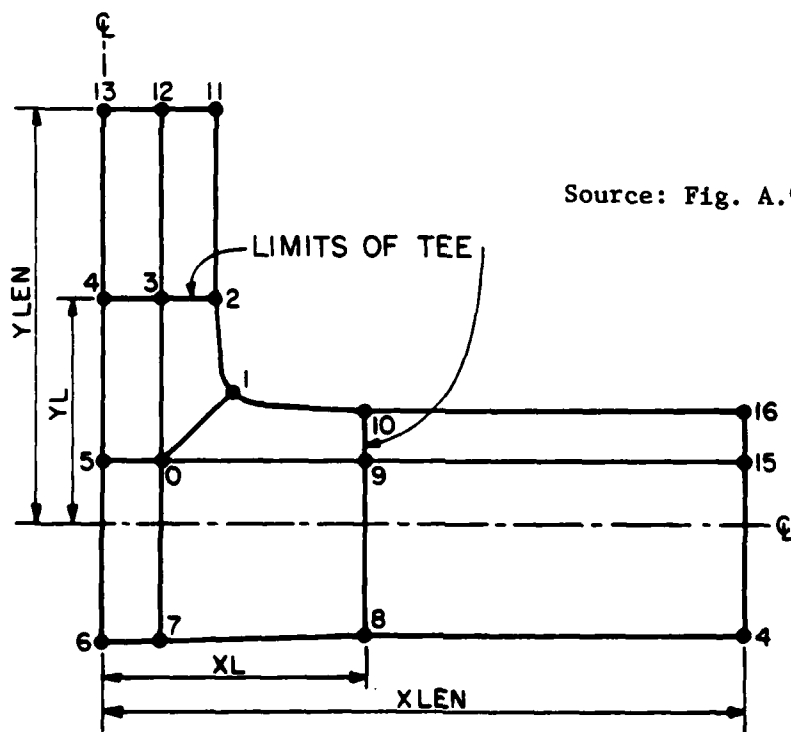


Figure 6 - Finite Element Model of Tee Using Idealized Geometry; Mesh 4



(a) Idealized Tee Geometry



(b) Control Nodes for Input of Thicknesses

Figure 7 - Geometry Input Parameters for Idealized Mesh Generation



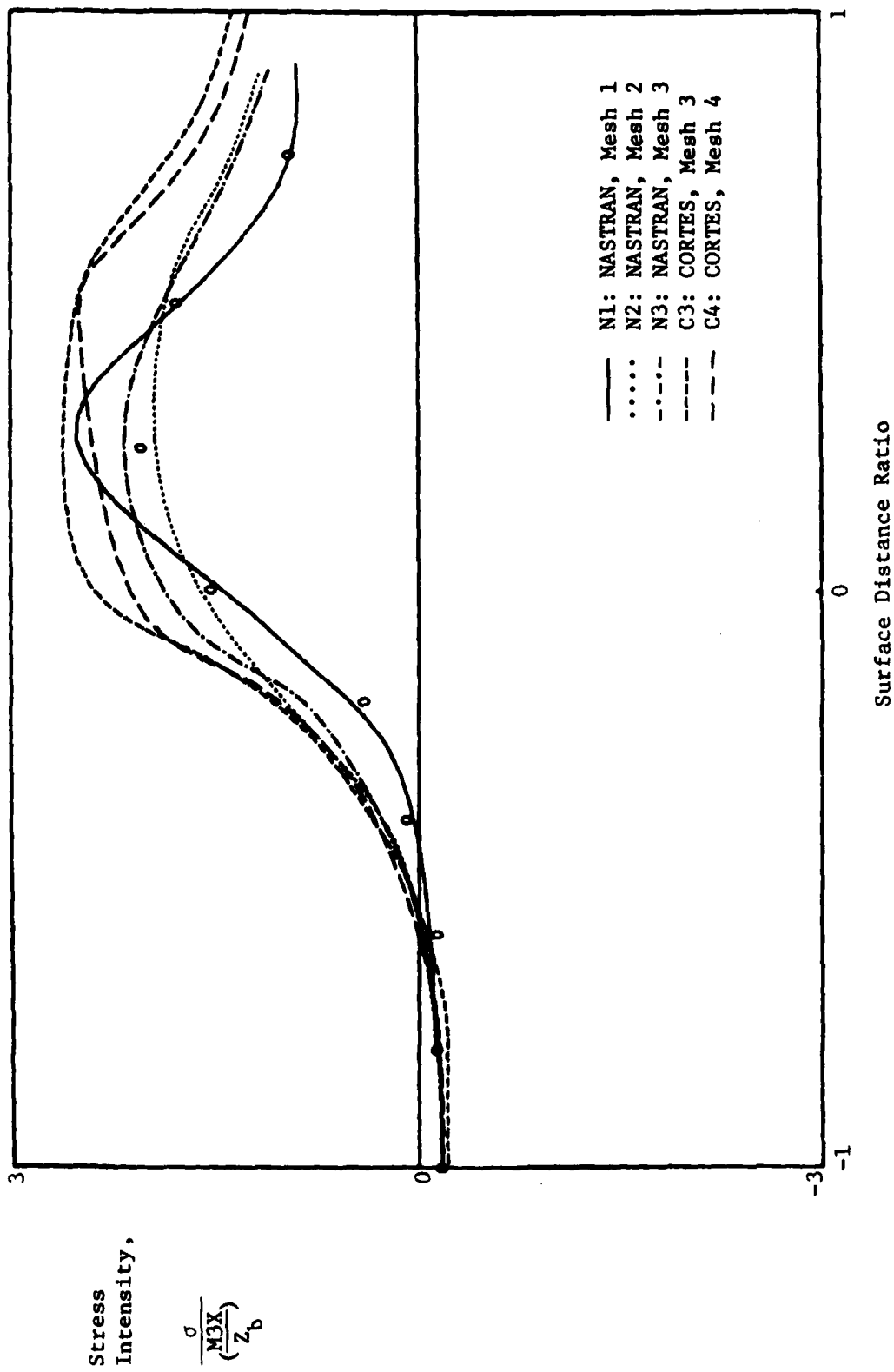


Figure 8 - Normalized Stress Intensity for Load Case 1 (M3X), Row 1, Major Principal Stress on Outer Surface

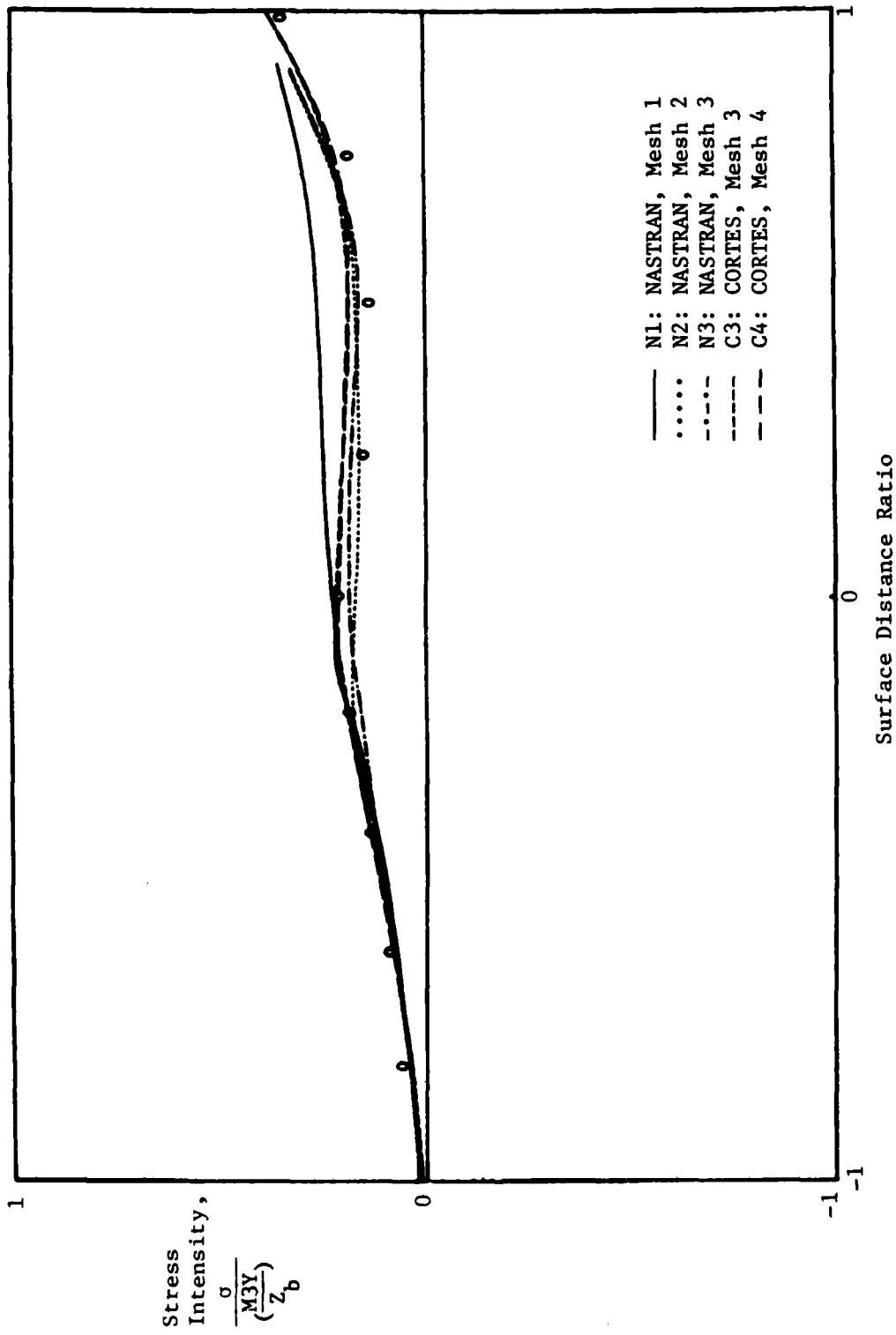


Figure 9 - Normalized Stress Intensity for Load Case 2 (M3Y), Row 1, Major Principal Stress on Outer Surface

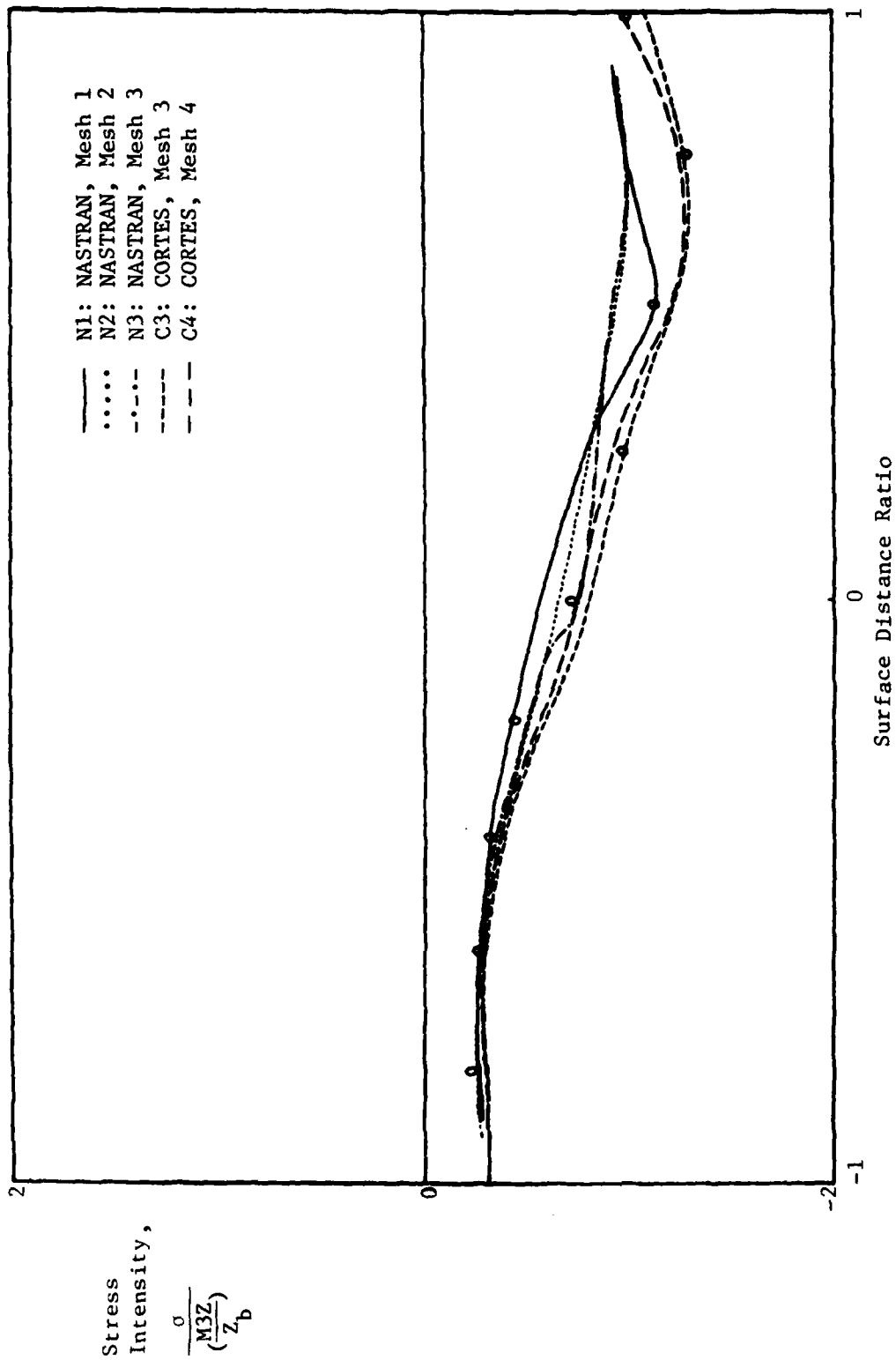


Figure 10 - Normalized Stress Intensity for Load Case 3 (M3Z), Row 6,  
Minor Principal Stress on Outer Surface

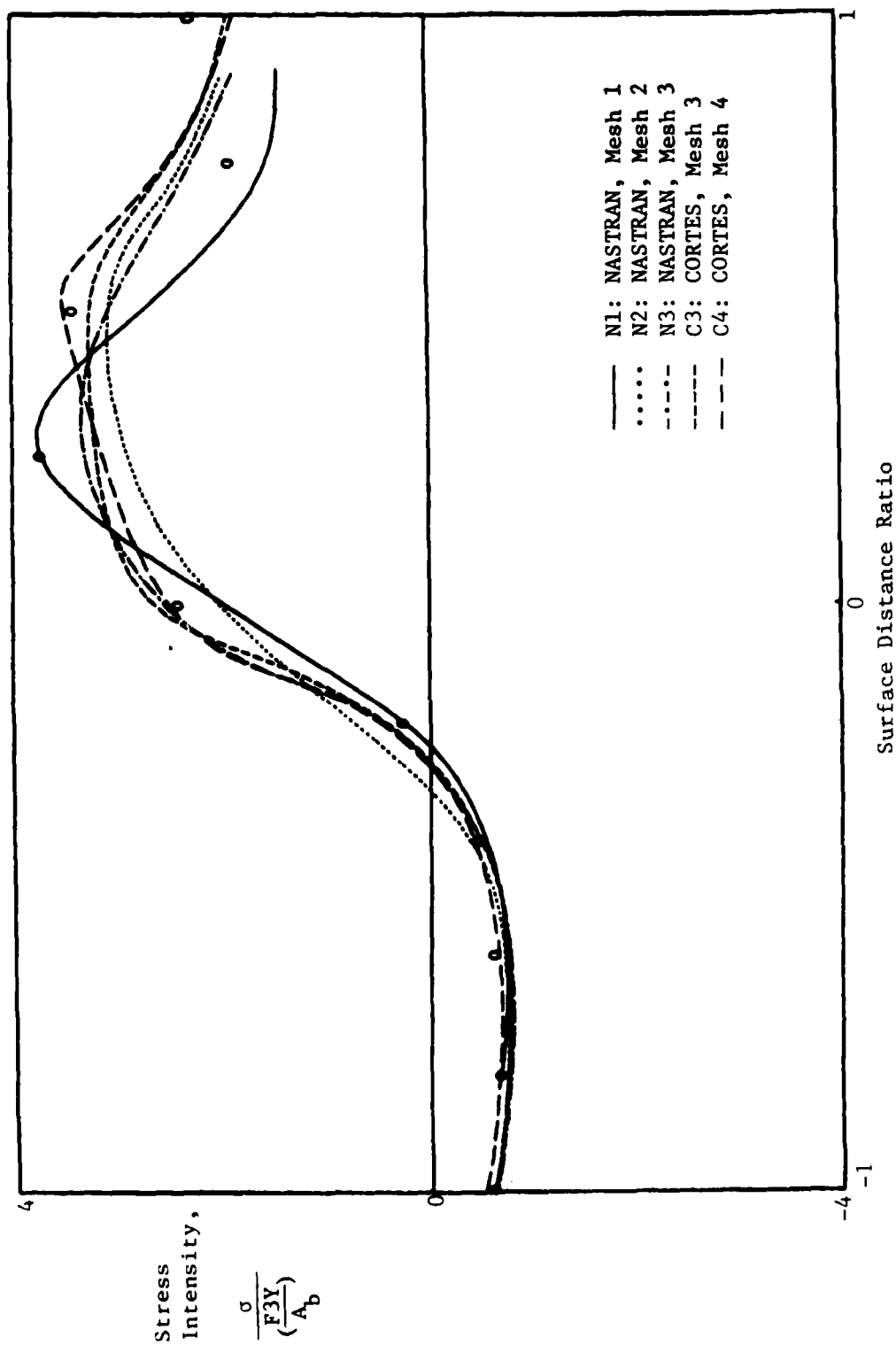


Figure 11 - Normalized Stress Intensity for Load Case 5 (F3Y), Row 1,  
Major Principal Stress on Outer Surface

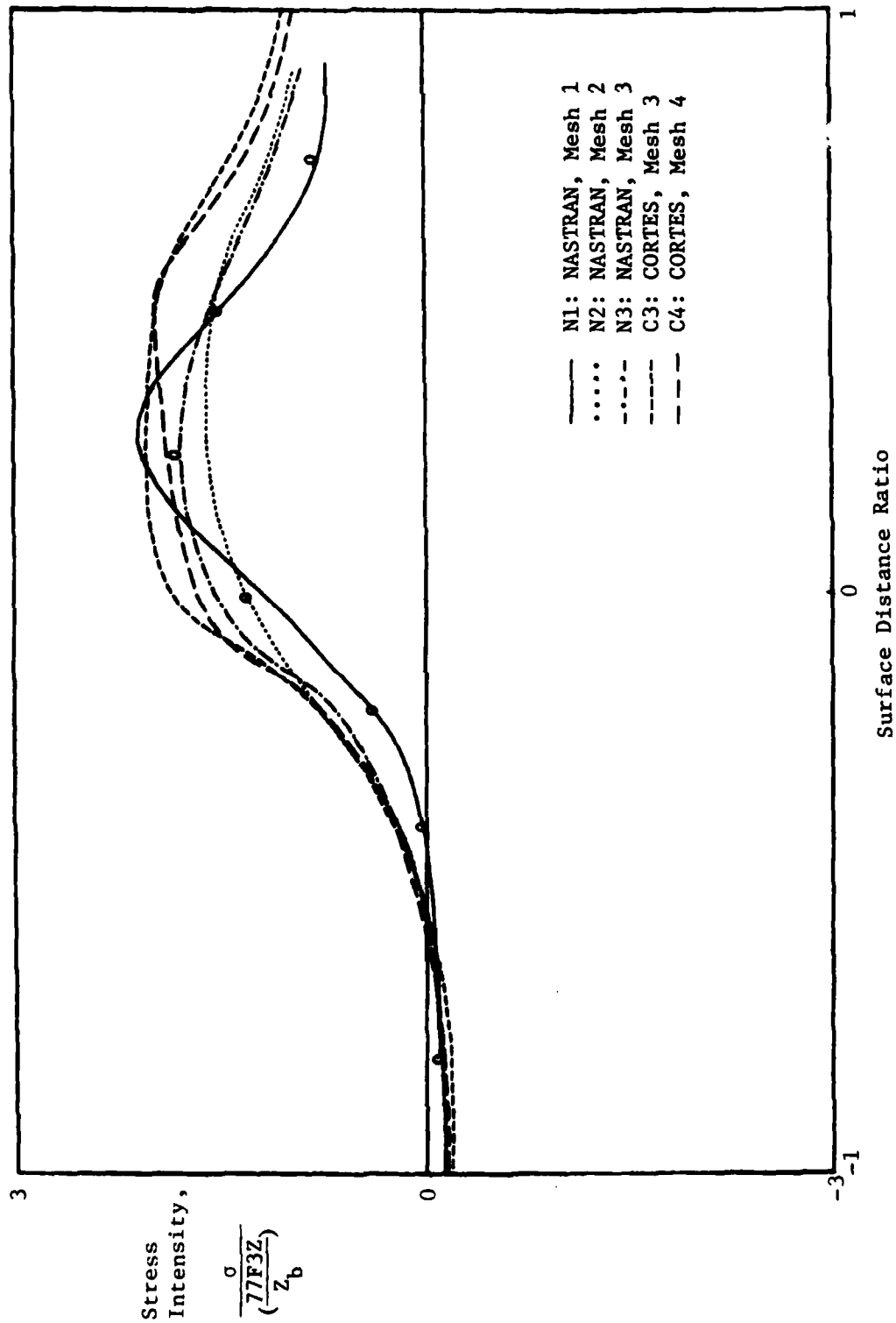


Figure 12 - Normalized Stress Intensity for Load Case 6 (F3Z), Row 1,  
Major Principal Stress on Outer Surface

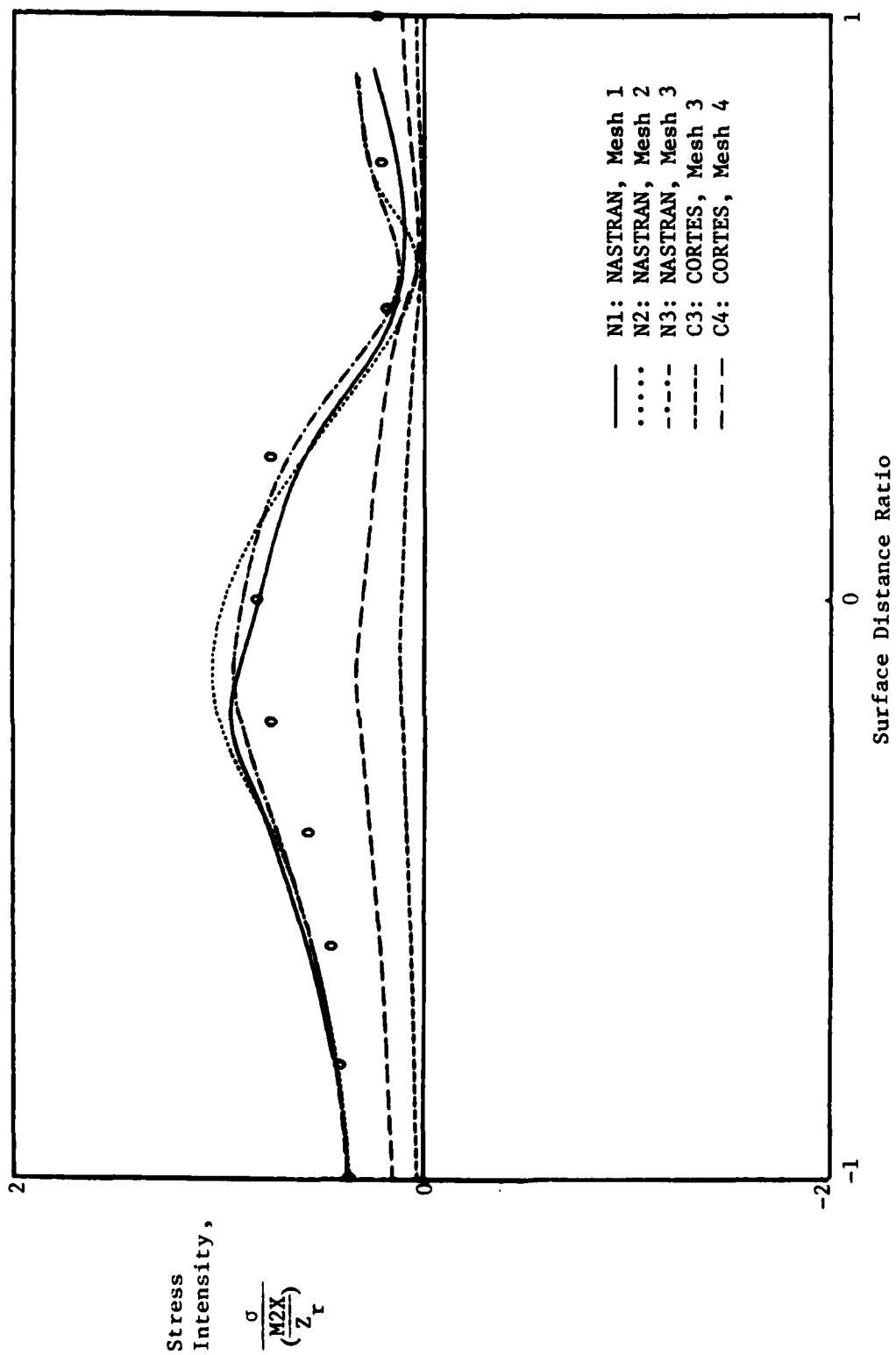


Figure 13 - Normalized Stress Intensity for Load Case 7 (M2X), Row 1,  
Major Principal Stress on Outer Surface

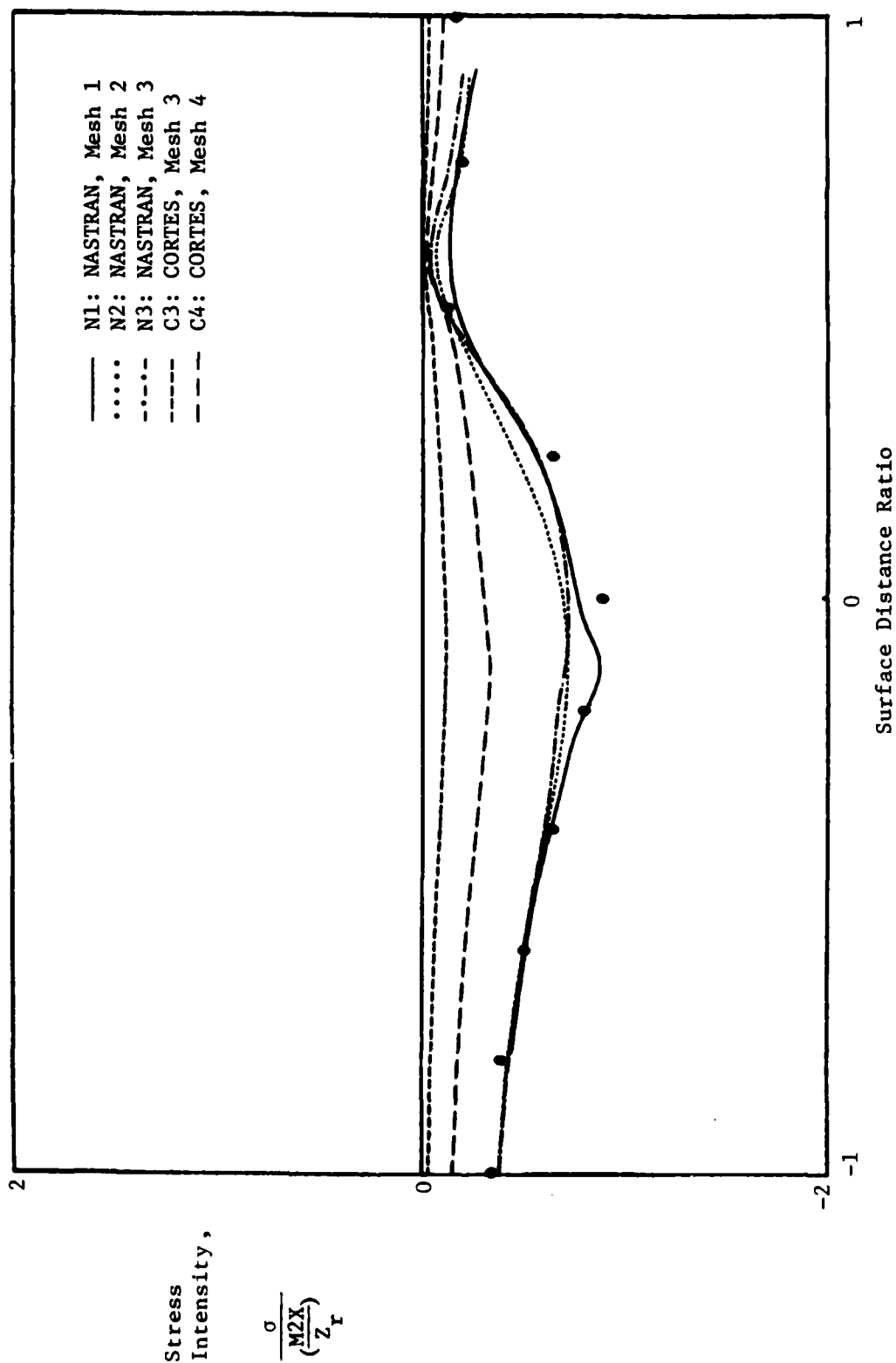


Figure 14 - Normalized Stress Intensity for Load Case 7 (M2X), Row 1,  
Minor Principal Stress on Outer Surface

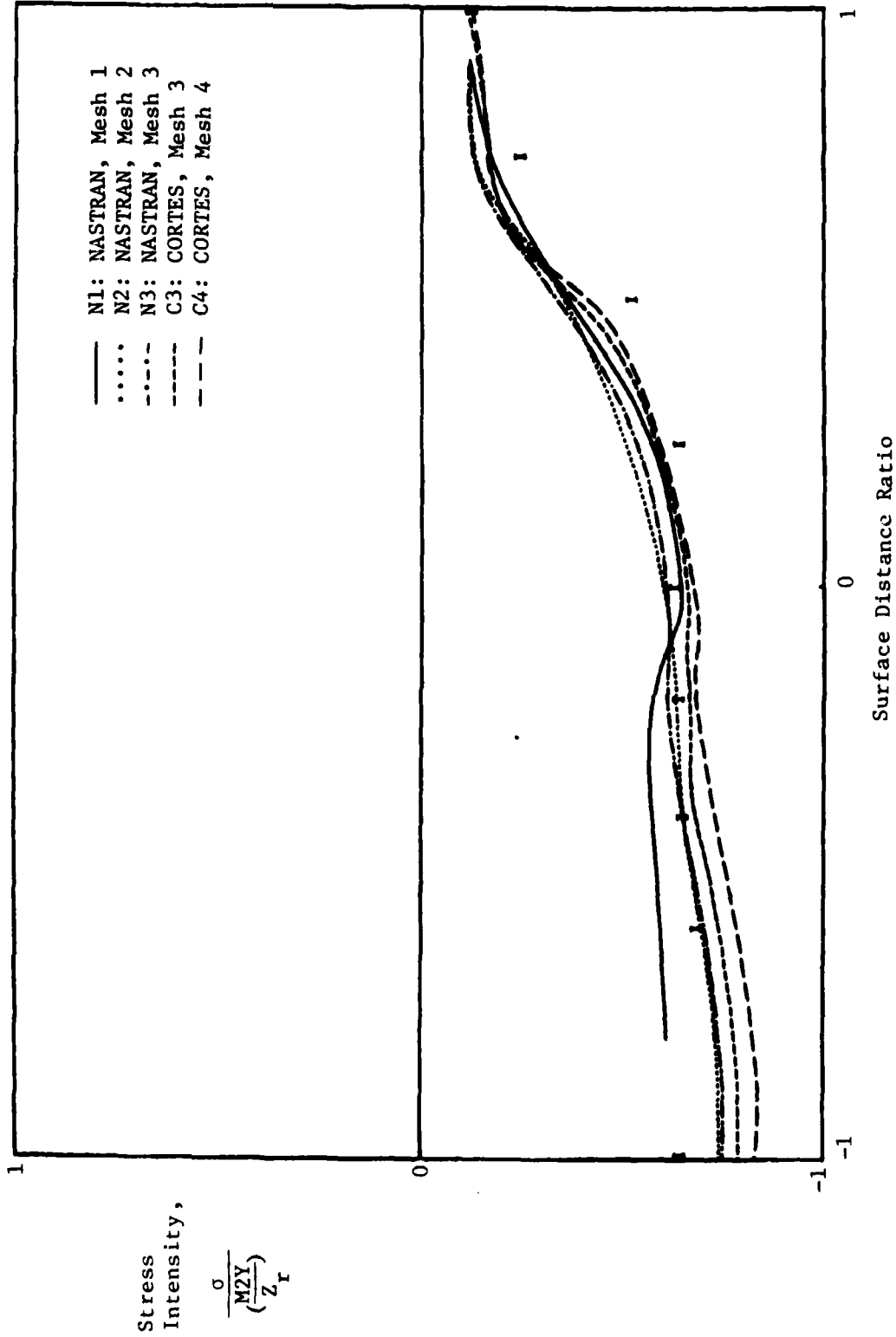


Figure 15 - Normalized Stress Intensity for Load Case 8 (M2Y), Row 1,  
Minor Principal Stress on Inner Surface



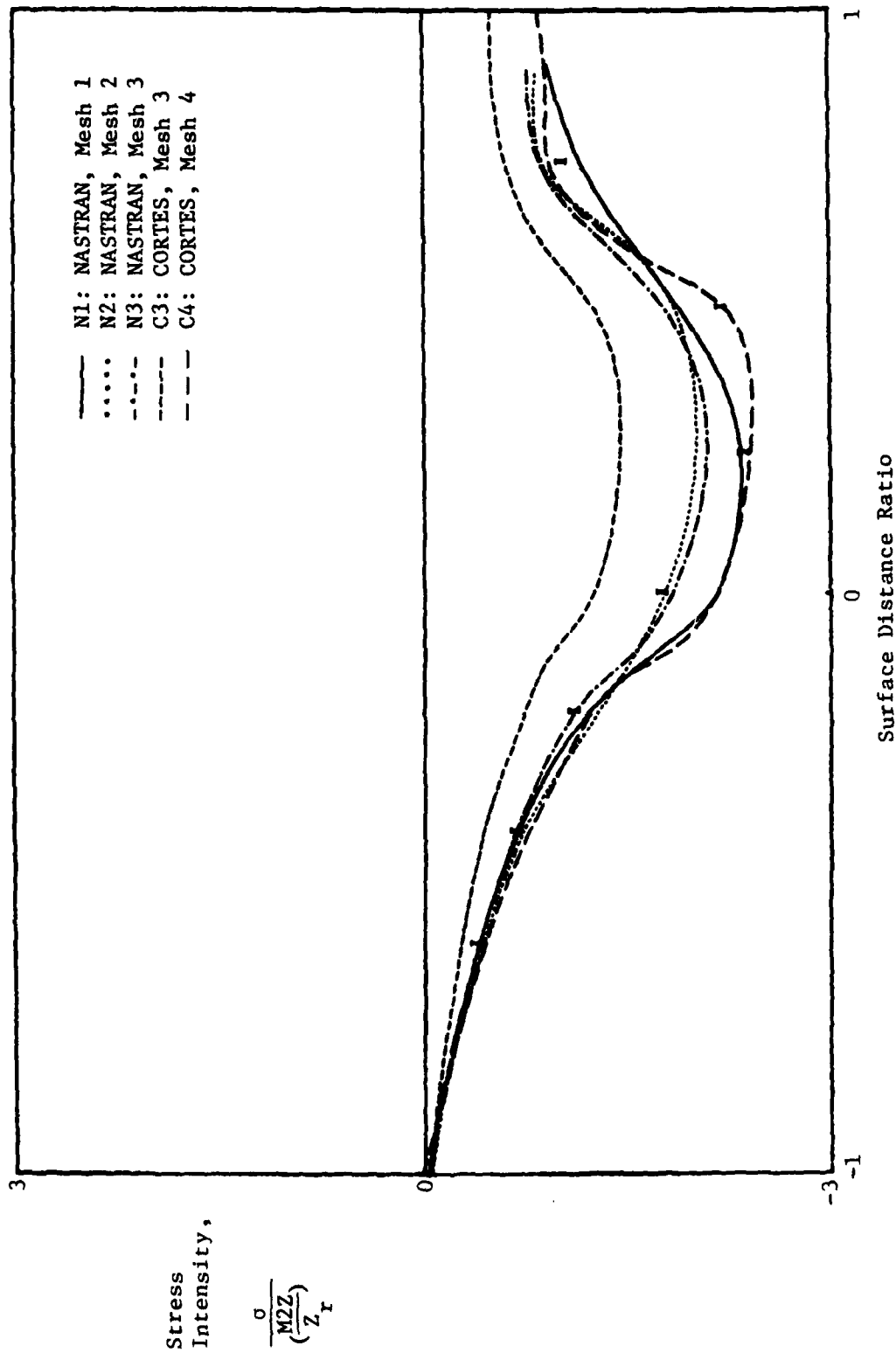


Figure 16 - Normalized Stress Intensity for Load Case 9 (M2Z), Row 1,  
Minor Principal Stress on Inner Surface

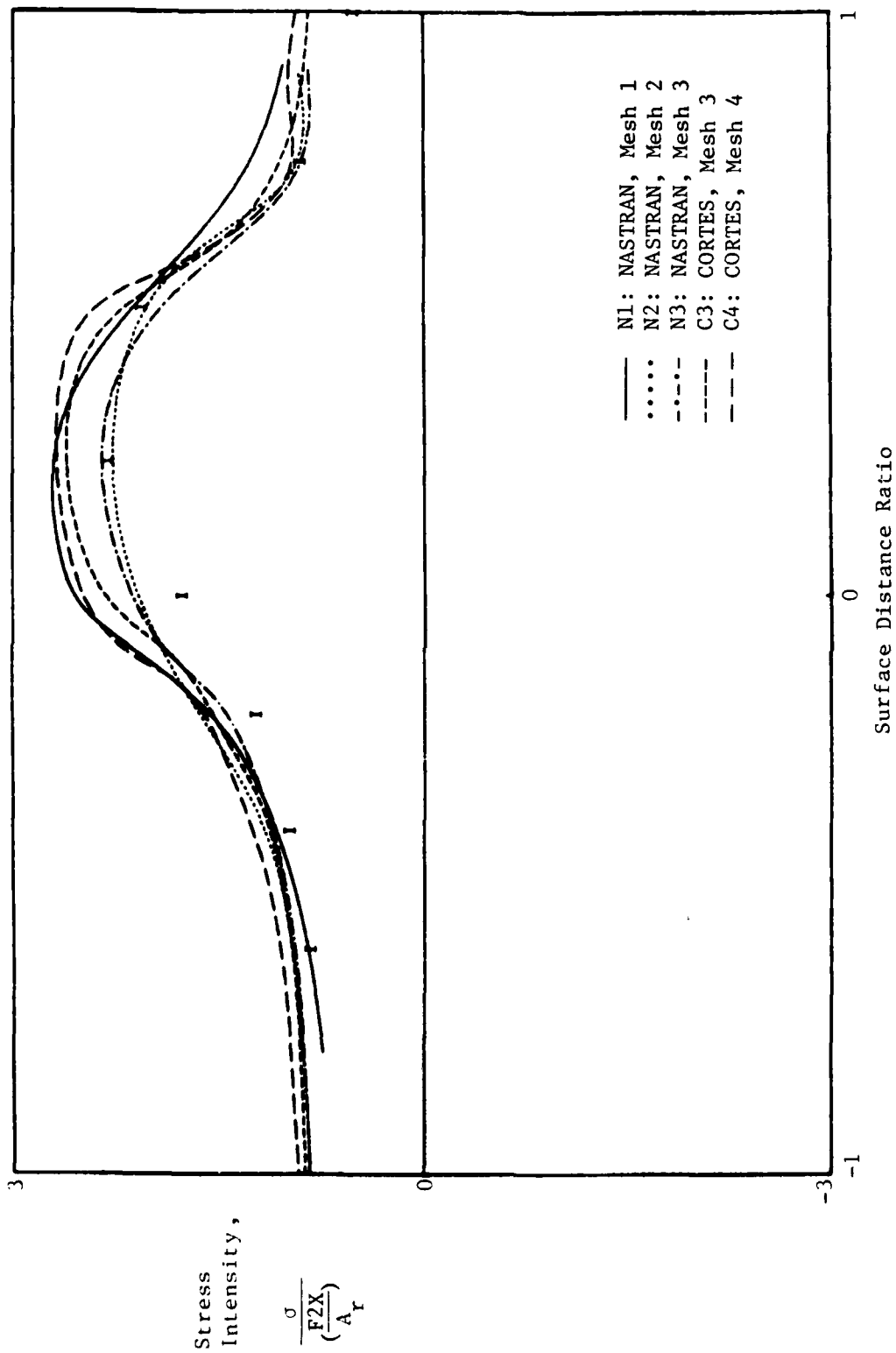


Figure 17 - Normalized Stress Intensity for Load Case 10 (F2X), Row 1,  
Major Principal Stress on Inner Surface

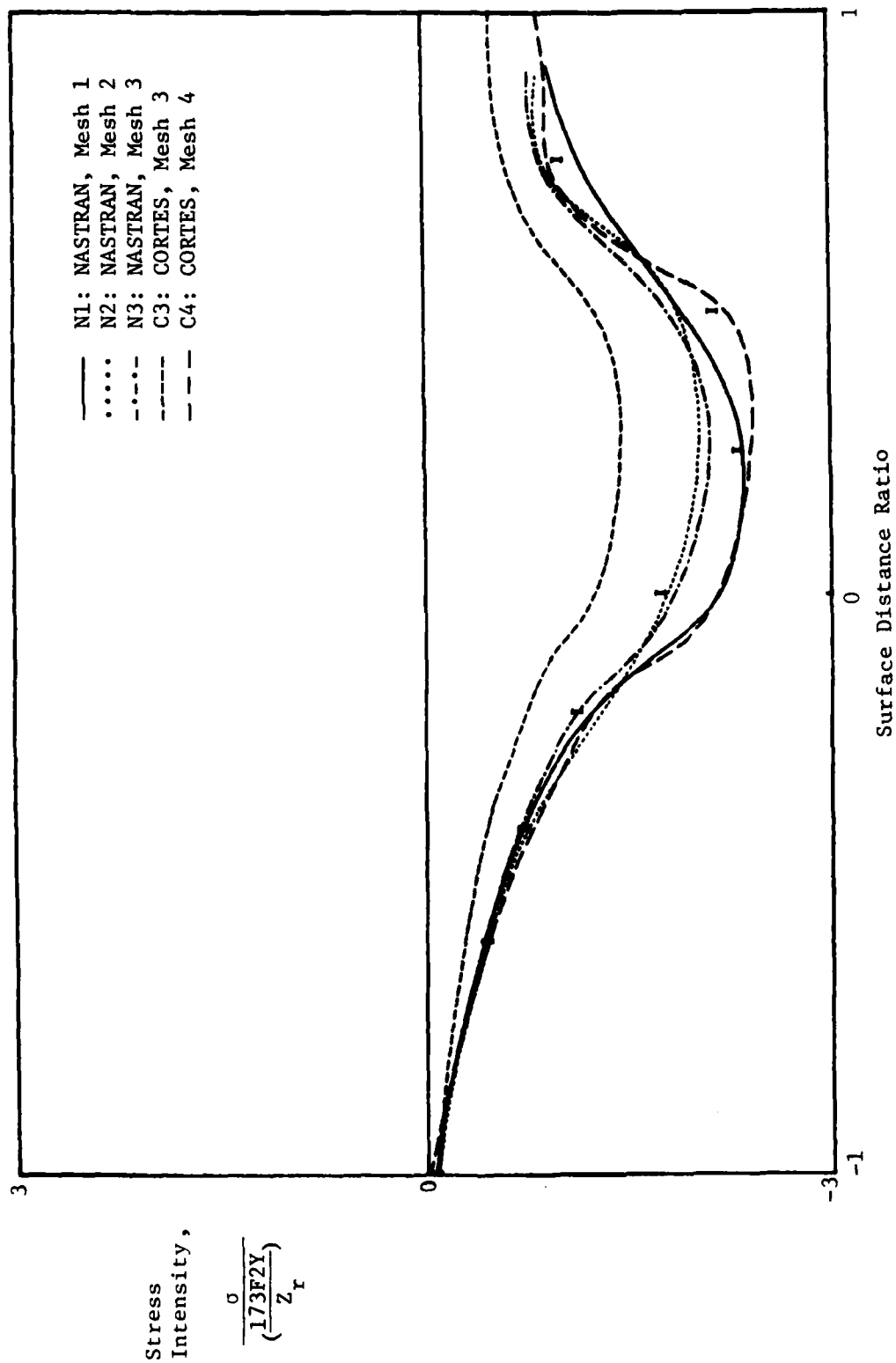


Figure 18 - Normalized Stress Intensity for Load Case 11 (F2Y), Row 1,  
Minor Principal Stress on Inner Surface

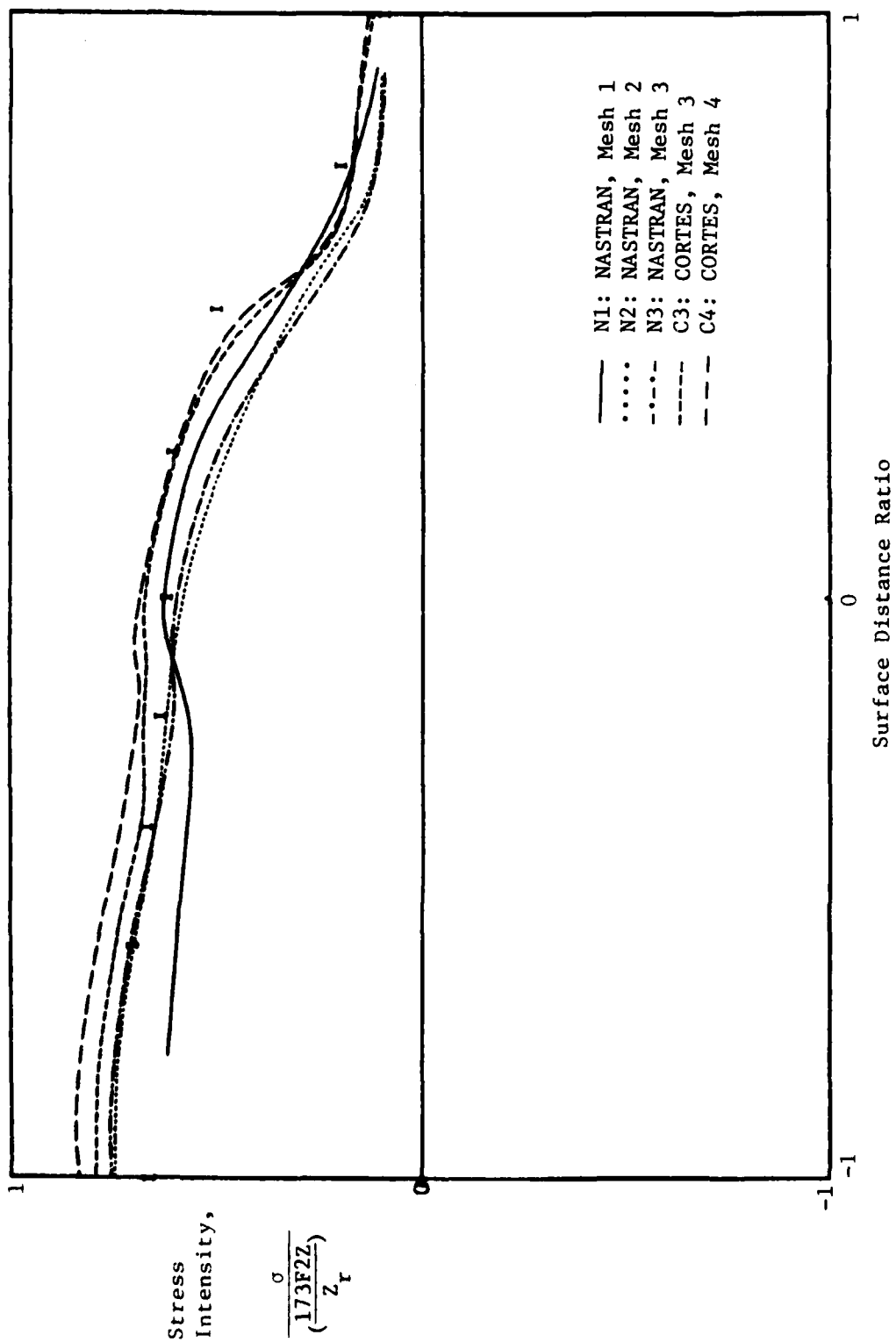


Figure 19 - Normalized Stress Intensity for Load Case 12 (F2Z), Row 1, Major Principal Stress on Inner Surface

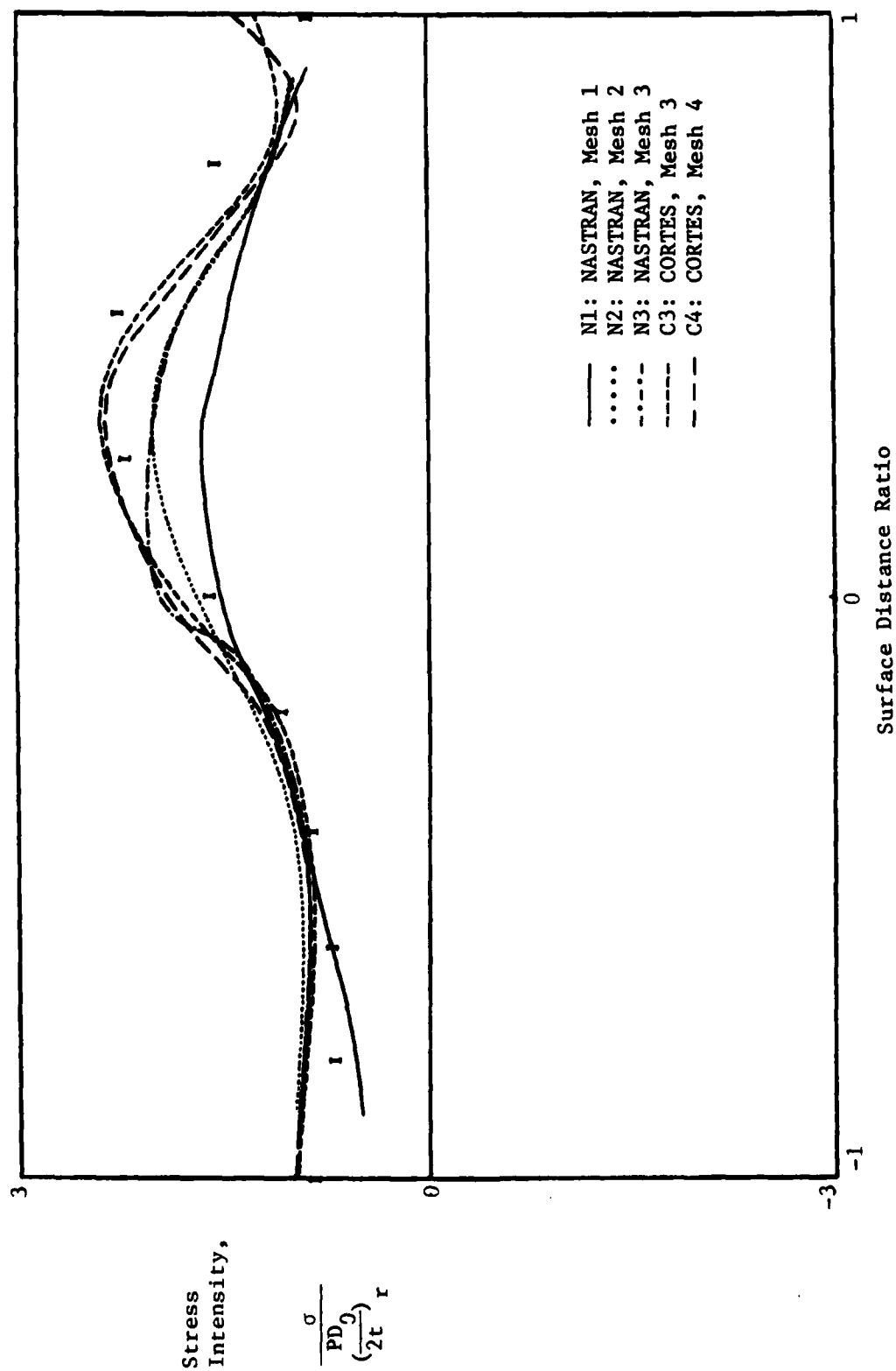


Figure 20 - Normalized Stress Intensity for Load Case 13 (P), Row 6,  
Major Principal Stress on Inner Surface

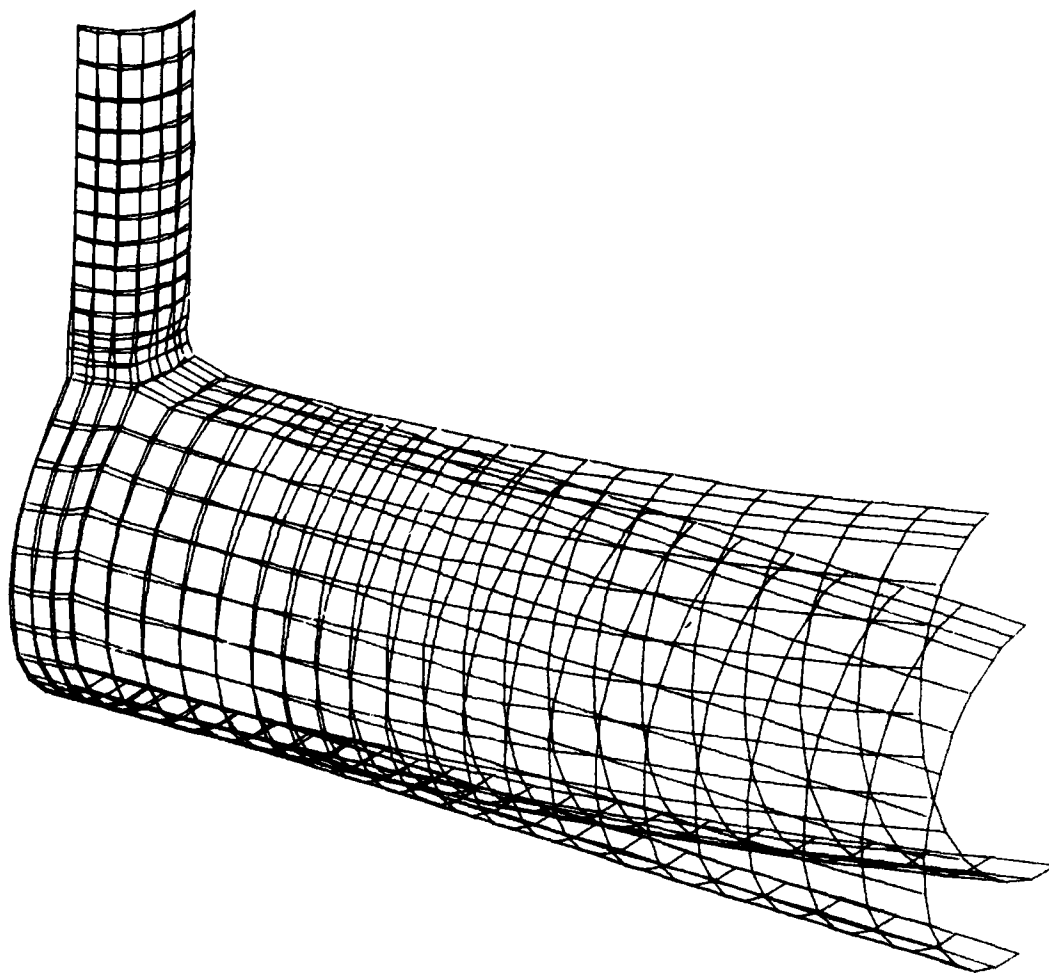


Figure 21 - Superimposed Plots of Undeformed and Deformed  
Tee Model Due to In-Plane Bending Moment  
on the Run (M2Z)

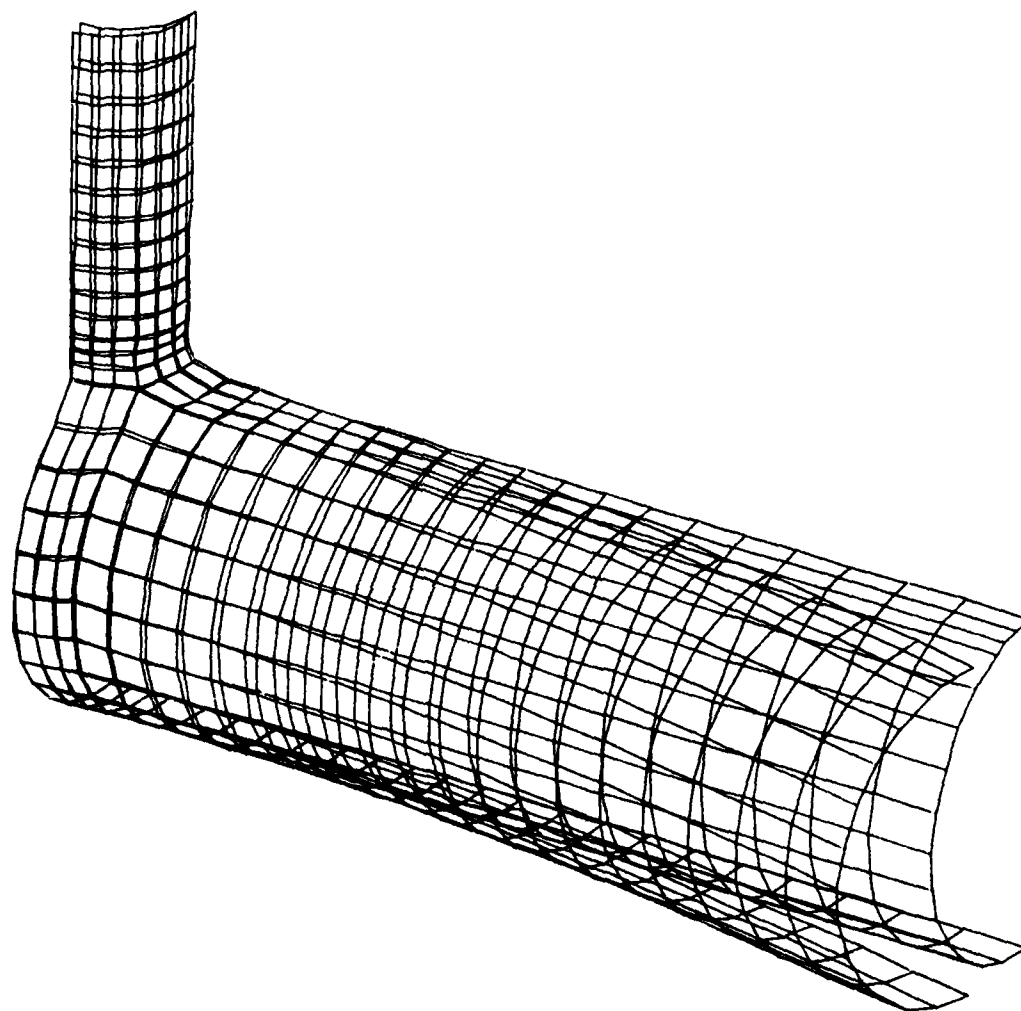


Figure 22 - Superimposed Plots of Undeformed and Deformed Tee  
Model Due to Out-of-Plane Bending Moment  
on the Run (M2Y)

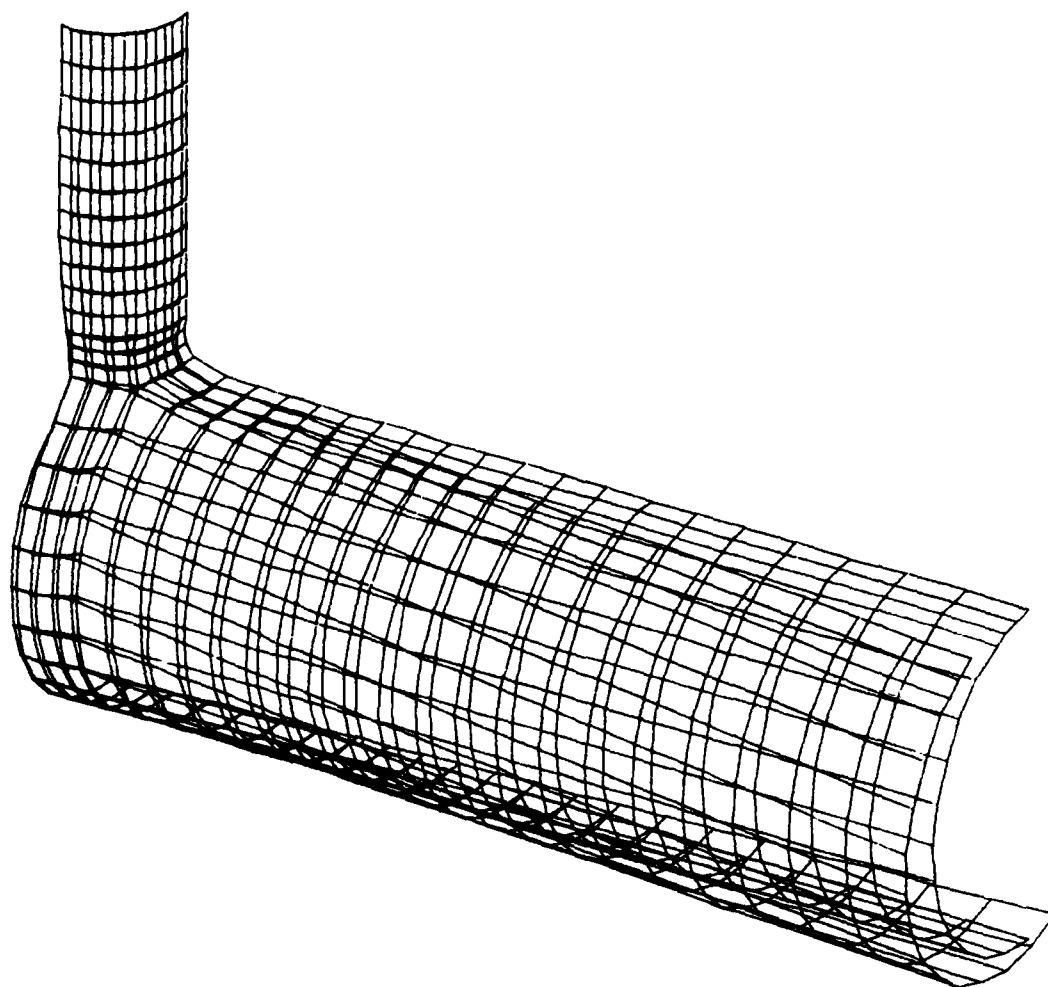


Figure 23 - Superimposed Plots of Undeformed and Deformed Tee Model Due to Torsional Moment on the Run (M2X)



#### REFERENCES

1. Marcus, M.S. and G.C. Everstine, "Finite Element Analysis of Pipe Elbows," Report CMLD-79/15, David W. Taylor Naval Ship Research and Development Center, Bethesda, Maryland (Feb 1980).
2. Gantayat, A.N. and G.H. Powell, "Stress Analysis of Tee Joints by the Finite Element Method," Report No. US SESM 73-6, Structural Engineering Laboratory, Univ. of California, Berkeley, California (Feb 1973).
3. Henley, D.R., "Test Report on Experimental Stress Analysis of a 24" Diameter Tee (ORNL T-12)," Report CENC 1237, ORNL-Sub-3310-4, Combustion Engineering, Inc., Chattanooga, Tennessee (Apr 1975).
4. Golden, M.E., "Geometric Structural Modelling: A Promising Basis for Finite Element Analysis," Trends in Computerized Structural Analysis and Synthesis, edited by A.K. Noor and H.B. McComb, Jr., Pergamon Press, Oxford, England, pp. 347-350 (May 1978).
5. Golden, M.E., "The Role of a Geometry Processor in Structural Analysis," New Techniques in Structural Analysis by Computer, edited by R. Melosh and M. Salama, Preprint 3601, ASCE Convention and Exposition (2-6 Apr 1979), American Society of Civil Engineers, Boston, MA, pp. F1-F17.
6. McKee, J.M. and R.J. Kazden, "G-Prime B-Spline Manipulation Package--Basic Mathematical Subroutines," DTNSRDC Report 77-0036, David W. Taylor Naval Ship Research and Development Center, Bethesda, Maryland (Apr 1977).
7. McKee, J.M., "Updates to the G-Prime B-Spline Manipulation Package--26 October 1977," periodic updates available from the author at the David W. Taylor Naval Ship Research and Development Center, Bethesda, Maryland 20084.

# INITIAL DISTRIBUTION

## Copies

### 13 NAVSEA

1 SEA 05D  
3 SEA 05D12  
1 SEA 05R  
2 SEA 05R14  
2 SEA 0532  
2 SEA 99612  
2 SEA 09G32/Lib

### 12 DTIC

1 Oak Ridge National Laboratory  
(Union Carbide Nuclear Div.)  
1 S.E. Moore  
  
1 Combustion Engineering, Inc.  
Chattanooga, TN  
1 J.K. Hayes

## CENTER DISTRIBUTION

Copies	Code	Name
1	18	G.H. Gleissner
2	1809.3	D. Harris
1	184	J.W. Schot
1	1844	S.K. Dhir
4	1844	G.C. Everstine
4	1844	A.J. Quezon
1	1844	M.E. Golden
1	27	W. Dietz
1	274	L. Argiro
1	2740	Y.F. Wang
2	2744	D. Allwein Y.P. Lu
5	2744	L. Kaldor
1	522.1	Unclassified Lib (C)
1	522.2	Unclassified Lib (A)

### **DTNSRDC ISSUES THREE TYPES OF REPORTS**

**1. DTNSRDC REPORTS, A FORMAL SERIES, CONTAIN INFORMATION OF PERMANENT TECHNICAL VALUE. THEY CARRY A CONSECUTIVE NUMERICAL IDENTIFICATION REGARDLESS OF THEIR CLASSIFICATION OR THE ORIGINATING DEPARTMENT.**

**2. DEPARTMENTAL REPORTS, A SEMIFORMAL SERIES, CONTAIN INFORMATION OF A PRELIMINARY, TEMPORARY, OR PROPRIETARY NATURE OR OF LIMITED INTEREST OR SIGNIFICANCE. THEY CARRY A DEPARTMENTAL ALPHANUMERICAL IDENTIFICATION.**

**3. TECHNICAL MEMORANDA, AN INFORMAL SERIES, CONTAIN TECHNICAL DOCUMENTATION OF LIMITED USE AND INTEREST. THEY ARE PRIMARILY WORKING PAPERS INTENDED FOR INTERNAL USE. THEY CARRY AN IDENTIFYING NUMBER WHICH INDICATES THEIR TYPE AND THE NUMERICAL CODE OF THE ORIGINATING DEPARTMENT. ANY DISTRIBUTION OUTSIDE DTNSRDC MUST BE APPROVED BY THE HEAD OF THE ORIGINATING DEPARTMENT ON A CASE-BY-CASE BASIS.**